AMERICAN SOCIETY FOR MICROBIOLOGY | mBio®

RESEARCH ARTICLE
Molecular Biology and Physiology

RstA Is a Major Regulator of *Clostridioides difficile* Toxin Production and Motility

Adrianne N. Edwards,[a] Brandon R. Anjuwon-Foster,[b]* Shonna M. McBride[a]

[a]Department of Microbiology and Immunology, Emory Antibiotic Resistance Center, Emory University School of Medicine, Atlanta, Georgia, USA
[b]Department of Microbiology and Immunology, University of North Carolina at Chapel Hill School of Medicine, Chapel Hill, North Carolina, USA

ABSTRACT *Clostridioides difficile* infection (CDI) is a toxin-mediated diarrheal disease. Several factors have been identified that influence the production of the two major *C. difficile* toxins, TcdA and TcdB, but prior published evidence suggested that additional unknown factors were involved in toxin regulation. Previously, we identified a *C. difficile* regulator, RstA, that promotes sporulation and represses motility and toxin production. We observed that the predicted DNA-binding domain of RstA was required for RstA-dependent repression of toxin genes, motility genes, and *rstA* transcription. In this study, we further investigated the regulation of toxin and motility gene expression by RstA. DNA pulldown assays confirmed that RstA directly binds the *rstA* promoter via the predicted DNA-binding domain. Through mutational analysis of the *rstA* promoter, we identified several nucleotides that are important for RstA-dependent transcriptional regulation. Further, we observed that RstA directly binds and regulates the promoters of the toxin genes *tcdA* and *tcdB*, as well as the promoters for the *sigD* and *tcdR* genes, which encode regulators of toxin gene expression. Complementation analyses with the *Clostridium perfringens* RstA ortholog and a multispecies chimeric RstA protein revealed that the *C. difficile* C-terminal domain is required for RstA DNA-binding activity, suggesting that species-specific signaling controls RstA function. Our data demonstrate that RstA is a transcriptional repressor that autoregulates its own expression and directly inhibits transcription of the two toxin genes and two positive toxin regulators, thereby acting at multiple regulatory points to control toxin production.

IMPORTANCE *Clostridioides difficile* is an anaerobic, gastrointestinal pathogen of humans and other mammals. *C. difficile* produces two major toxins, TcdA and TcdB, which cause the symptoms of the disease, and forms dormant endospores to survive the aerobic environment outside the host. A recently discovered regulatory factor, RstA, inhibits toxin production and positively influences spore formation. Herein, we determine that RstA directly binds its own promoter DNA to repress its own gene transcription. In addition, our data demonstrate that RstA directly represses toxin gene expression and gene expression of two toxin gene activators, TcdR and SigD, creating a complex regulatory network to tightly control toxin production. This study provides a novel regulatory link between *C. difficile* sporulation and toxin production. Further, our data suggest that *C. difficile* toxin production is regulated through a direct, species-specific sensing mechanism.

KEYWORDS *Clostridium*, *Clostridium difficile*, RNPP, RRNPP, TcdA, TcdB, helix-turn-helix, motility, spore, sporulation, toxin, transcriptional regulator

Clostridioides difficile infection (CDI) is a nosocomial and community-acquired gastrointestinal disease that affects individuals with dysbiotic gut microbiota, which commonly occurs after antibiotic treatment (1, 2). Clinical outcomes range from mild diarrhea to severe disease symptoms, including sepsis and death (1). The two glyco-

Citation Edwards AN, Anjuwon-Foster BR, McBride SM. 2019. RstA is a major regulator of *Clostridioides difficile* toxin production and motility. mBio 10:e01991-18. https://doi.org/10.1128/mBio.01991-18.

Editor Bruce A. McClane, University of Pittsburgh School of Medicine

Address correspondence to Shonna M. McBride, shonna.mcbride@emory.edu.

* Present address: Brandon R. Anjuwon-Foster, Laboratory of Molecular Biology, Cell Biology Section, National Cancer Institute, National Institutes of Health, Bethesda, Maryland, USA.

Received 10 September 2018
Accepted 25 January 2019
Published 12 March 2019

sylating exotoxins, TcdA and TcdB, elicit CDI symptoms and are indispensable for *C. difficile* virulence (3). Environmental and intracellular signals, including nutrient availability and metabolic cues, strongly influence toxin production (4–7). There are numerous identified *C. difficile* factors that control toxin gene expression in response to these signals (8–12); however, the regulatory pathways and molecular mechanisms that directly control toxin gene expression are not fully understood (13).

Our previous work identified a novel regulator, RstA, which depresses *C. difficile* toxin production and motility (14). RstA inhibits transcription of the toxin genes *tcdA* and *tcdB*, the toxin-specific sigma factor, *tcdR*, and the flagellum-specific sigma factor, *sigD*, which is essential for motility and directs *tcdR* expression (11, 12, 14–16). In addition to repressing motility and toxin production, RstA positively influences *C. difficile* spore formation, which is critical for the survival of the bacterium outside of the host and for transmission from host to host, indicating that RstA regulates diverse phenotypes important for *C. difficile* pathogenesis. An *rstA* mutant exhibits increased toxin gene expression *in vivo* and is more virulent in the hamster model of CDI, demonstrating the impact RstA has on pathogenesis (14).

The predicted secondary structure of RstA reveals three apparent domains: an N-terminal conserved helix-turn-helix DNA-binding domain, followed by a series of multiple tetratricopeptide repeat (TPR) domains comprising a putative Spo0F-like protein-binding domain, and a C-terminal putative quorum-sensing-like domain (14). These characteristic features place RstA in the RRNPP (Rap/Rgg/NprR/PlcR/PrgX; formerly RNPP) family of proteins. RRNPP proteins are prevalent in Gram-positive organisms and regulate competence, sporulation, toxin production, and other important survival and virulence phenotypes (17–19). The DNA-binding or protein-binding activity of RRNPP proteins are controlled by the direct binding of small, quorum-sensing peptides (19). The precursor proteins encoding the quorum-sensing peptides are often adjacent to the regulatory RRNPP protein and are translated, exported, processed, and reinternalized at high cell densities (20–25). In addition, RRNPP proteins often autoregulate their own expression, as is observed for RstA (14). The presence of these conserved domains within RstA provides insight into how RstA may regulate *C. difficile* toxin production, motility, and sporulation.

To better understand the regulatory impact RstA exerts on *C. difficile* toxin production and sporulation, we examined the function of the conserved DNA-binding domain. Our previous study (14) had shown that the DNA-binding domain is required for RstA-dependent regulation of *rstA* expression and toxin gene expression but is expendable for sporulation regulation. Here, we demonstrate that RstA directly binds to its promoter via an imperfect inverted repeat and that it directly binds the *sigD* and toxin gene promoters. Further, our data demonstrate that RstA and SigD independently control toxin expression, creating a multitiered regulatory pathway by which RstA represses toxin production. Finally, we show that the *Clostridium perfringens rstA* ortholog does not complement toxin production or sporulation in a *C. difficile rstA* mutant. However, a chimeric RstA protein containing the *C. perfringens* DNA-binding domain and the *C. difficile* Spo0F-binding and quorum-sensing-binding domains restores sporulation and represses toxin production, providing evidence that the ability to respond to species-specific signaling is necessary for RstA DNA-binding activity.

RESULTS

RstA autoregulates its gene transcription via an inverted repeat overlapping the promoter. Our previous work provided preliminary genetic evidence that the N-terminal putative helix-turn-helix DNA-binding domain was necessary for inhibition of toxin gene expression but was dispensable for sporulation initiation (14). However, further work with the recombinant His-tagged RstA proteins revealed that the constructs were expressed at low levels and were not detected by Western blotting of *C. difficile* lysates (data not shown). We created a new series of tagged proteins, possessing the 3×FLAG tag on the C-terminal end and found that these were stably expressed and easily detected in *C. difficile rstA*::*erm* lysates (see Fig. S2A in the supplemental

material). Corroborating our previous data (14), expression of the wild-type RstA, the full-length FLAG-tagged RstA, and the truncated RstAΔHTH-FLAG-tagged allele complemented sporulation in the *rstA* mutant (Fig. S2B). As previously observed (14), only full-length RstA restored toxin production to wild-type levels in the *rstA* background (Fig. S2C and D), confirming that the helix-turn-helix motif within the DNA-binding domain is essential for RstA-dependent control of toxin production.

We hypothesized that RstA directly binds to DNA to control toxin gene expression and transcription of additional target genes. This interaction is predicted to occur via the putative DNA-binding domain, as observed for other RRNPP transcriptional regulators (26–28). Additionally, we previously observed that *rstA* expression remains relatively unchanged throughout growth in multiple conditions and that *rstA* transcription is increased in an *rstA* mutant (14), suggesting that expression of *rstA* may be autoregulated. To determine whether RstA is DNA-binding protein, we first defined the *rstA* promoter region and probed the DNA-binding capability of RstA within its own promoter. The transcriptional start of *rstA* was identified at −32 bp upstream from the translational start using 5′ RACE. Corresponding σ^A −10 and −35 consensus sequences were detected immediately upstream of this transcriptional start site (Fig. 1A and B). To verify the mapped promoter and to determine whether any additional promoters are present that drive *rstA* transcription, a series of promoter fragments fused to the *phoZ* reporter gene was created, and alkaline phosphatase (AP) activity was measured in the 630Δ*erm* and *rstA*::*erm* mutants. As previously observed, the full-length 489-bp *rstA* promoter fragment exhibited a 1.8-fold increase in activity in the *rstA* mutant compared to the parent strain, indicating RstA-dependent repression (Fig. 1C) (14). The truncated promoter fragments, P*rstA*$_{291}$ and P*rstA*$_{231}$, produced similar fold changes in activity in the *rstA* mutant and parent strains, as observed for the full-length promoter. However, reporter activity was lower in the P*rstA*$_{115}$ fragment compared to the longer fragments, suggesting that an enhancer sequence or an additional RstA-independent transcriptional activator is located between −231 bp to −115 bp upstream of the *rstA* open reading frame. A promoter fragment reporter fusion containing 380 bp of sequence upstream from the mapped *rstA* promoter [from −489 bp to −112 bp; intergenic region (IR) in Fig. 1A] was inactive, indicating that an additional promoter is not located within this region. We also tested whether RstA-dependent repression of the full-length P*rstA* reporter could be complemented. We expressed the *rstA*-FLAG construct from the nisin-inducible promoter, *cprA* (29), divergently from the P*rstA*::*phoZ* construct on the same plasmid in the *rstA*::*erm* background. P*rstA* reporter activity was reduced in a dose-dependent manner relative to the amount of nisin added to the medium (Fig. S3), further confirming the autoregulatory effect RstA exerts on its own expression. Altogether, the data demonstrate that the mapped σ^A-dependent promoter drives *rstA* expression and that RstA can repress transcription from this promoter.

The results obtained from the promoter-reporter fusions suggested that RstA binding was likely to occur within the 115 bp upstream of the translational start site. A 29-bp imperfect inverted repeat was identified within the predicted P*rstA* −10 consensus sequence, suggesting a possible regulatory binding site within this region (Fig. 1B). To determine whether this sequence serves as an RstA recognition site, we created a series of single nucleotide substitutions within the inverted repeat in the 489-bp P*rstA* reporter fusion, avoiding conserved residues required for RNAP-holoenzyme recognition (30). Most of the single nucleotide substitutions did not significantly alter reporter activity compared to the wild-type P*rstA* reporter (Fig. 1D). However, nucleotide substitutions in two positions, A-21 and T-19, abolished RstA repression in the parent strain, increasing reporter activity to match that of the *rstA*::*erm* mutant. These data suggest that the A-21 and T-19 nucleotides are important for RstA binding to the *rstA* promoter.

RstA inhibits toxin and motility gene transcription. Regulatory control of toxin gene expression in *C. difficile* involves multiple sigma factors and transcriptional regulators, which ensure that toxin production occurs in the appropriate environmental conditions (13). Our previous work (14) demonstrated that an *rstA*::*erm* mutant has

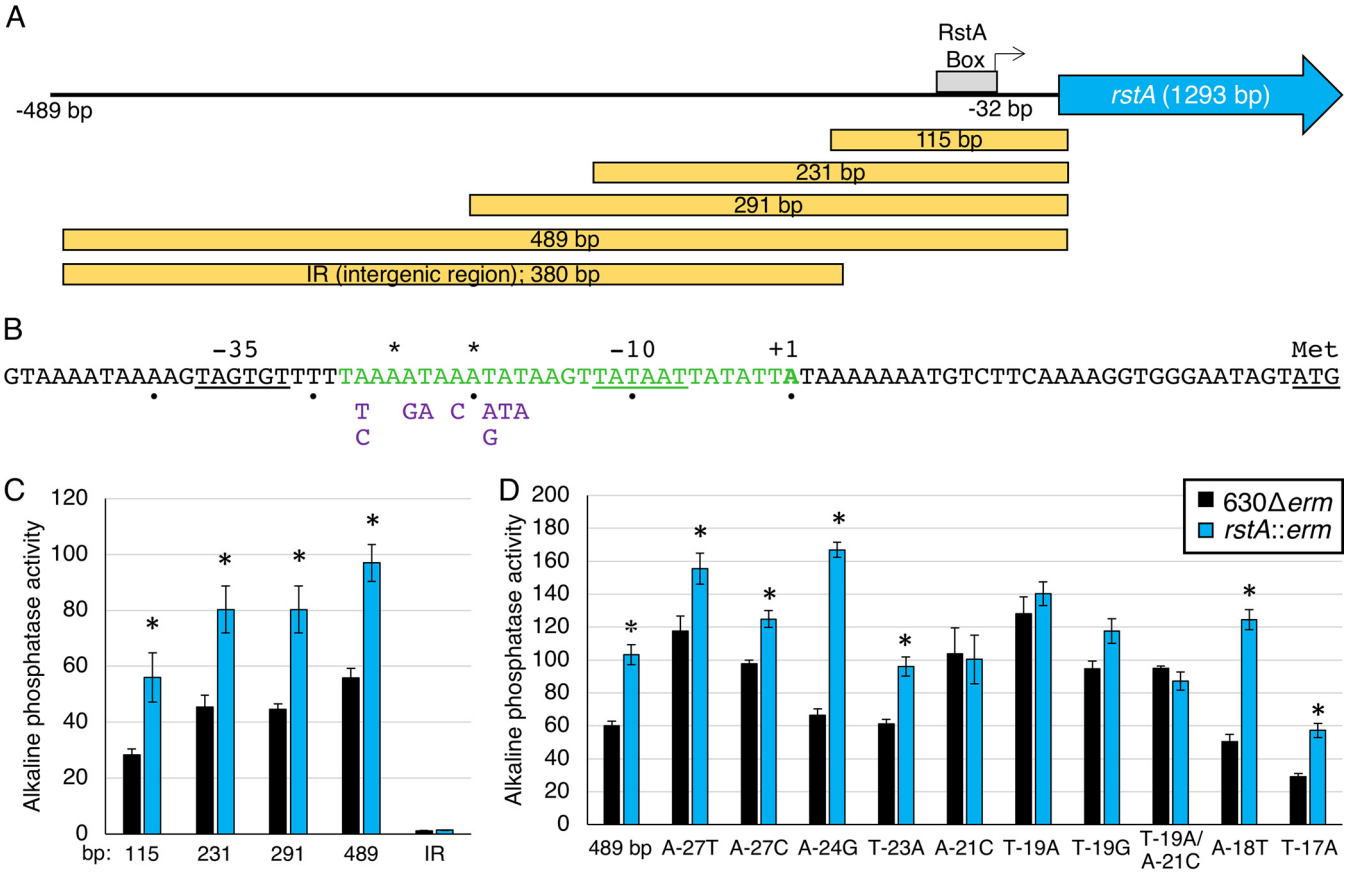

FIG 1 RstA controls its gene expression through an inverted repeat sequence overlapping the *rstA* promoter. (A) A schematic of the *rstA* promoter region denoting the general location of the putative RstA box, the transcriptional start (32 bp upstream from the start codon; represented by the bent arrow), and the *rstA* open reading frame (not to scale). The yellow boxes indicate the locations and sizes of promoter fragments constructed for the *phoZ* reporter fusions in panel C. (B) The *rstA* promoter, marked by +1, overlaps a 29-bp imperfect inverted repeat (shown in green). The asterisks above the sequence mark the mismatched nucleotides within the inverted repeat. The −10 and −35 consensus sequences and the ATG start codon are underlined. The nucleotides below the sequence represent the substitutions tested in panel D. (C and D) Alkaline phosphatase (AP) activity of the P*rstA*::*phoZ* reporter fusions of various lengths, including the upstream intergenic region (IR) (−489 bp to −112 relative to the translational start) of *rstA* (C) (P$rstA_{115}$ [MC979/MC980]), P$rstA_{231}$ [MC1010/MC1011], P$rstA_{291}$ [MC1012/MC1013], P$rstA_{489}$ [MC773/MC774], P$rstA_{IR}$ [MC1008/MC1009]) or of the full-length P*rstA*::*phoZ* promoter with various nucleotide substitutions (D) (P$rstA_{489}$ [MC773/MC774], P$rstA_{A\text{-}27T}$ [MC830/MC831], P$rstA_{A\text{-}27C}$ [MC856/MC857], P$rstA_{A\text{-}24G}$ [MC858/MC859], P$rstA_{T\text{-}23A}$ [MC832/MC833], P$rstA_{A\text{-}21C}$ [MC860/MC861], P$rstA_{T\text{-}19A}$ [MC834/MC835], P$rstA_{T\text{-}19G}$ [MC862/MC863], P$rstA_{T\text{-}19A/A\text{-}21C}$ [MC1433/1434], P$rstA_{A\text{-}18T}$ [MC836/MC837], P$rstA_{T\text{-}17A}$ [MC838/MC839]) in strain 630Δ*erm* and the *rstA*::*erm* mutant (MC391), respectively, grown on 70:30 sporulation agar at H_8. The means ± standard errors of the means for four biological replicates are shown. Values that are significantly different ($P < 0.05$) by Student's *t* test from the activity observed for the 630Δ*erm* parent strain for each promoter construct are indicated by an asterisk.

increased transcription of the *C. difficile* toxin genes, *tcdA* and *tcdB*, the toxin-specific sigma factor, *tcdR*, and the flagellum-specific sigma factor, *sigD*, which is required for motility and directs *tcdR* transcription (11, 12). To determine whether RstA is involved directly in repressing transcription of these genes, we first constructed *phoZ* reporter fusions with the promoter regions for each gene and examined RstA-dependent transcriptional activity.

The *tcdR* promoter region contains four identified independent promoter elements: a σ^A-dependent promoter (−16 bp from the translational start), a σ^D-dependent promoter (−76 bp from the translational start), and two putative σ^{TcdR} promoters farther upstream (Fig. 2A) (11, 12, 31–33). Expression of the *tcdR* gene is relatively low in *C. difficile* (11, 32, 34), at least in part due to repression by CodY and CcpA binding throughout the *tcdR* promoter region under nutrient-rich conditions (8, 9, 33, 35, 36). We examined each of the promoter elements within P*tcdR* to determine whether RstA affects transcription from these promoters. A series of reporter fusions was created for each of the promoter elements, which were examined in the *rstA*::*erm* mutant and parent strain, and activity was measured after 24 h of growth in TY medium (Fig. 2A).

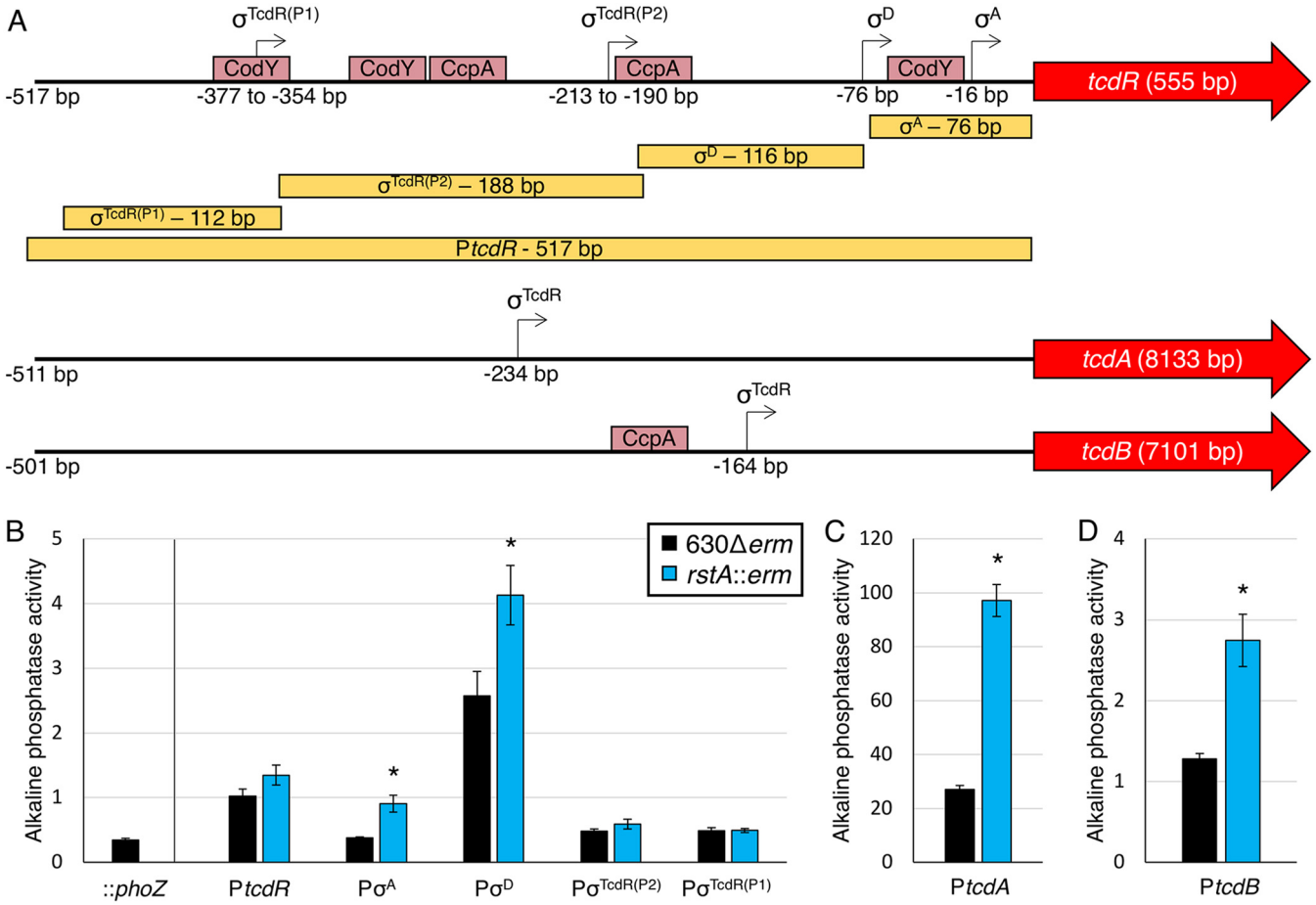

FIG 2 RstA inhibits toxin gene expression. (A) A schematic of the promoter regions of *tcdR*, *tcdA*, and *tcdB* denoting the relative locations of the transcriptional start sites experimentally demonstrated (12, 32–34) and the open reading frames of all three genes (not drawn to scale). Pale red boxes approximate CodY- and CcpA-binding sites within the toxin gene promoters (8, 9, 36). The yellow boxes indicate the locations and sizes of the promoter fragments constructed for the *phoZ* reporter fusions in panels B to D. Alkaline phosphatase (AP) activity of the P*tcdR*::*phoZ* reporter fusions of various lengths (B) (promoterless *phoZ* [MC448], P$tcdR_{\sigma A}$ [MC1285/MC1286], P$tcdR_{\sigma D}$ [MC1145/MC1146], P$tcdR_{\sigma TcdR(P2)}$ [MC1147/MC1148], and P$tcdR_{\sigma TcdR(P1)}$ [MC1149/MC1150]) and the P*tcdA*::*phoZ* (C) (−511 bp to −1 bp upstream of transcriptional start; MC1249/MC1250) or P*tcdB*::*phoZ* (D) (−531 bp to −31 bp upstream of transcriptional start [MC1251/MC1252]) reporter fusions in strain 630Δ*erm* and the *rstA*::*erm* mutant (MC391) grown in TY medium (pH 7.4) at H_{24}. The means and standard errors of the means for four biological replicates are shown. *, $P < 0.05$, using Student's *t* test compared to the activity observed in the 630Δ*erm* parent strain for each promoter construct.

A full-length 517-bp P*tcdR*::*phoZ* reporter and the two σ^{TcdR}-dependent promoter fusions exhibited similar low reporter activities in the parent and *rstA* strains (Fig. 2B). However, increased reporter activity was observed in the *rstA* mutant for the individual σ^{A}-dependent and σ^{D}-dependent promoter fusions. These results indicate that RstA impacts the function of these promoter elements and contributes to repression of *tcdR* transcription.

We also examined RstA-dependent regulation of *tcdA* and *tcdB* transcription, both of which are expressed solely from σ^{TcdR}-dependent promoters (Fig. 2A) (34, 37, 38). P*tcdA* reporter activity was increased 3.6-fold and P*tcdB* activity was 2.1-fold greater in the *rstA* strain compared to the parent (Fig. 2C and D). Altogether, these data indicate that RstA represses toxin gene transcription at the individual gene level and through repression of *tcdR*.

SigD, also known as FliA or σ^{28}, is a sigma factor that coordinates flagellar gene expression and directly activates *tcdR* gene expression (32). The *sigD* gene is located in a large, early-stage flagellar operon that is transcribed from a σ^{A}-dependent promoter located 496 bp upstream from the first gene of the *flgB* operon (39). Interestingly, the *flgB* promoter sequences from two different *C. difficile* strains, the historical epidemic

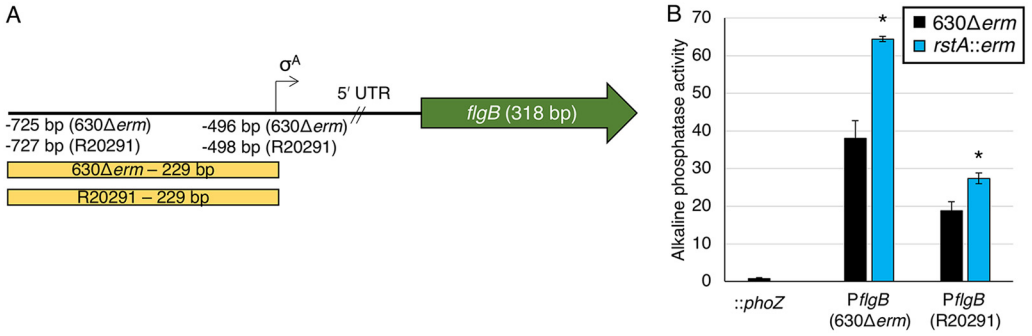

FIG 3 RstA represses expression of *flgB* reporter fusions. (A) A schematic of the *flgB* promoter regions for *C. difficile* 630 and R20291 strains. The transcriptional start site for the σ^A-dependent promoter for strain 630 lies −496 bp upstream from the *flgB* translational start, while the R20291 strain initiates transcription −498 bp upstream (39, 56). (B) Alkaline phosphatase (AP) activity of the promoterless::*phoZ* vector in 630Δ*erm* (MC1106) and P*flgB*$_{630\Delta erm}$::*phoZ* (MC1294/MC1295) and P*flgB*$_{R20291}$::*phoZ* (MC1296/MC1297) reporter fusions in 630Δ*erm* and the *rstA*::*erm* mutant (MC391) grown in TY medium (pH 7.4) at T_3 (three hours after the start of transition phase [OD_{600} of 1.0]). The means and standard errors of the means for three biological replicates are shown. *, $P < 0.05$, using Student's *t* test compared to the activity observed in the 630Δ*erm* parent strain for each promoter construct.

strain, strain 630, and a current epidemic strain, strain R20291, are identical to the σ^A promoter sequence through the translational start site but diverge considerably upstream of this region (Fig. S4). No additional promoter elements were identified in the strain 630 or R20291 sequences upstream of the σ^A-dependent promoter (Fig. 3A). To determine whether RstA influences *sigD* transcription through repression of P*flgB*, promoter reporter fusions representing each strain were constructed. As anticipated, activity of the strain 630Δ*erm* and R20291 P*flgB* reporters were higher in the *rstA* mutant than in the parent strain (1.7-fold and 1.5-fold, respectively; Fig. 3B), indicating that RstA represses *flgB* and consequently, *sigD* transcription.

RstA directly binds the *rstA*, *tcdR*, *flgB*, *tcdA*, and *tcdB* promoters via the conserved helix-turn-helix DNA-binding domain. To determine whether RstA directly binds target DNA, a variety of *in vitro* electrophoretic gel shift assays were attempted, but no binding was observed in any condition tested. We considered that the lack of RstA-DNA interaction by gel shift may occur because of the absence of a cofactor, such as a quorum-sensing peptide, or because of a transient complex or oligomerization state. To overcome this obstacle, we performed biotin-labeled DNA pulldown assays to assess the DNA-binding capacity of RstA under native conditions. Biotinylated DNA was coupled to streptavidin beads as bait and incubated with cell lysates expressing either full-length RstA-FLAG or RstAΔHTH-FLAG protein. Specifically bound proteins were eluted and analyzed by Western blotting using FLAG M2 antibody.

We first tested the ability of RstA to directly interact with its own promoter. RstA-FLAG protein was recovered using the wild-type *rstA* promoter region as bait, demonstrating specific interaction of the RstA protein (Fig. 4A). However, the P*rstA* fragment did not capture RstAΔHTH-FLAG protein, indicating that the conserved HTH domain of RstA is essential for DNA binding. In addition to the wild-type *rstA* promoter, the P*rstA* T-19A and P*rstA* A-21C variants that eliminated RstA-dependent regulation *in vivo* were used as bait (Fig. 1D). Both the P*rstA* T-19A and P*rstA* T-19A/A-21C variants captured significantly less RstA-FLAG than the wild-type promoter, suggesting that at least the T-19A nucleotide facilitates RstA interaction (Fig. 4A and Fig. S5A). The intergenic region upstream of the *rstA* promoter (Fig. 1A, IR) did not recover the full-length RstA-FLAG, indicating that RstA recognizes a specific DNA sequence within the promoter region. Finally, RstA-FLAG did not interact with unlabeled streptavidin beads nonspecifically (Fig. 4A and Fig. S5A). Altogether, these data demonstrate that RstA functions as a DNA-binding protein that directly and specifically binds its own promoter to repress transcription.

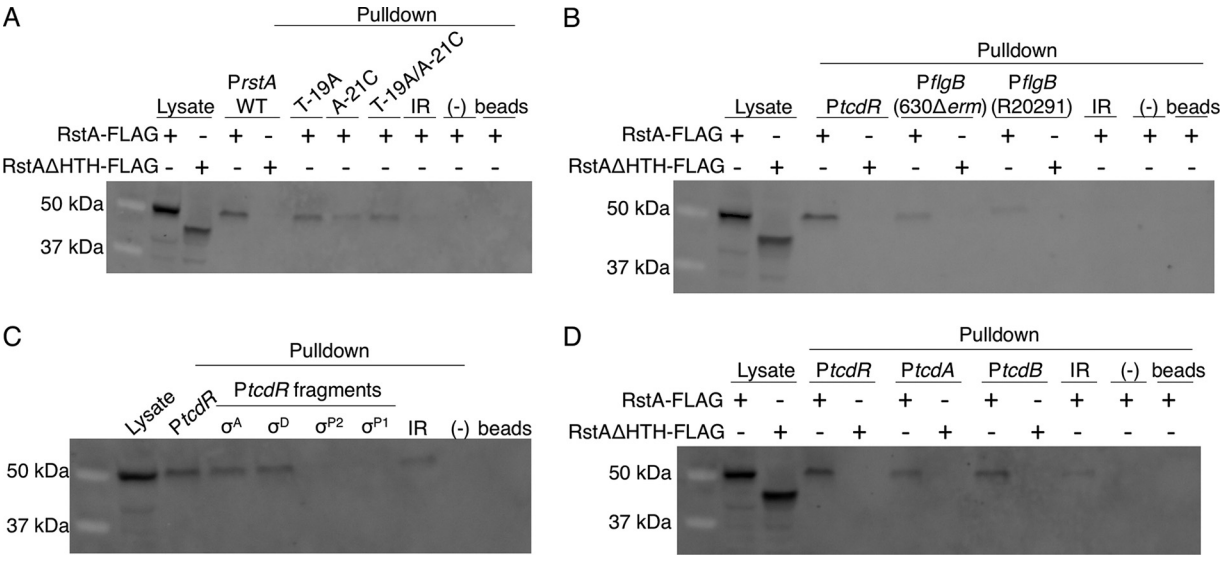

FIG 4 RstA binds to the *rstA*, *tcdR*, *flgB*, *tcdA*, and *tcdB* promoters. Western blot analysis using FLAG M2 antibody to detect recombinant RstA-3XFLAG or RstAΔHTH-3XFLAG in cell lysates or following biotin-labeled DNA pulldown assays. As a control, cell lysate expressing the RstA-3XFLAG construct (MC1004) or the RstAΔHTH-3XFLAG construct (MC1028) is included in the first lane or two of each Western blot shown. Additional negative controls in each panel include unbiotinylated full-length *rstA* promoter (−) and beads-only controls to ensure that RstA does not interact with the beads nonspecifically. The biotin-labeled fragments used as bait are of the 115-bp wild-type, T-19A, A-21C, or T-19A/A-21C *rstA* promoters or of the 380-bp intergenic region upstream of the *rstA* promoter (IR; see Fig. 2; present in all panels) (A), the full-length *tcdR* (446-bp) or the 630Δ*erm* or R20291 *flgB* (229-bp) promoters (B), the full-length *tcdR* (446-bp), σ^A-dependent (92-bp), σ^D-dependent (116-bp), σ^{TcdRP2}-dependent (188-bp), or σ^{TcdRP1}-dependent (112-bp) promoters (C), or the full-length *tcdR* (446-bp), *tcdA* (511-bp), or *tcdB* (501-bp) promoters (D). All promoter fragments were bound to streptavidin-coated magnetic beads and incubated with *C. difficile* cell lysates grown in TY medium (pH 7.4) supplemented with 2 μg/ml thiamphenicol and 1 μg/ml nisin to mid-log phase (OD_{600} of 0.5 to 0.7), expressing either the RstA-3XFLAG construct (MC1004) or the RstAΔHTH-3XFLAG construct (MC1028).

To determine whether RstA directly binds DNA to repress the transcription of genes encoding toxin regulators, we examined RstA binding to the *flgB* and *tcdR* promoter regions. RstA-FLAG protein bound specifically to the full-length *tcdR* promoter region, as well as the 630 and R20291 *flgB* promoters (Fig. 4B and Fig. S5B). Again, the HTH domain was required for these RstA-promoter interactions. To identify which internal promoter elements directly interact with RstA, previously characterized *tcdR* promoter fragments were used as bait (Fig. 2B), with the exception of a longer σ^A-dependent promoter fragment (92 bp rather than 76 bp) to limit potential steric hindrance of RstA binding due to the 5′ biotin label. This longer 92-bp P*tcdR*(σ^A) fragment exhibited the same RstA-dependent regulation in reporter assays as the 76-bp reporter (Fig. S6). RstA-FLAG bound to the σ^A-dependent and σ^D-dependent *tcdR* promoter fragments but was not recovered from either of the σ^{TcdR}-dependent promoters (Fig. 4C and Fig. S5B), corroborating the reporter fusion results that demonstrated RstA repression of only the σ^A-dependent and σ^D-dependent *tcdR* promoter elements.

DNA pulldown assays were also performed to ascertain whether RstA directly binds to the *tcdA* and *tcdB* promoters. Both of the toxin promoters captured the full-length RstA-FLAG protein and failed to recover the RstAΔHTH-FLAG protein (Fig. 4D and Fig. S5B). These data provide direct biochemical evidence that RstA represses *flgB*, *tcdR*, *tcdA*, and *tcdB* transcription by binding to the promoter regions of these genes.

RstA represses toxin gene expression independently of SigD-mediated toxin regulation. Our data indicate that RstA represses toxin gene expression directly by binding to the *tcdA* and *tcdB* promoter regions and indirectly by repressing transcription of the sigma factors *tcdR* and *sigD*, which activate toxin gene expression. The biotin pulldown data suggest that RstA represses toxin gene expression through a multitiered regulatory pathway. To test whether direct repression of *tcdA* and *tcdB* transcription by RstA is physiologically relevant and independent of SigD, we created an *rstA sigD* double mutant and examined the impact of each mutation on toxin production. To aid in construction of an *rstA sigD* double mutant, we utilized the recently developed

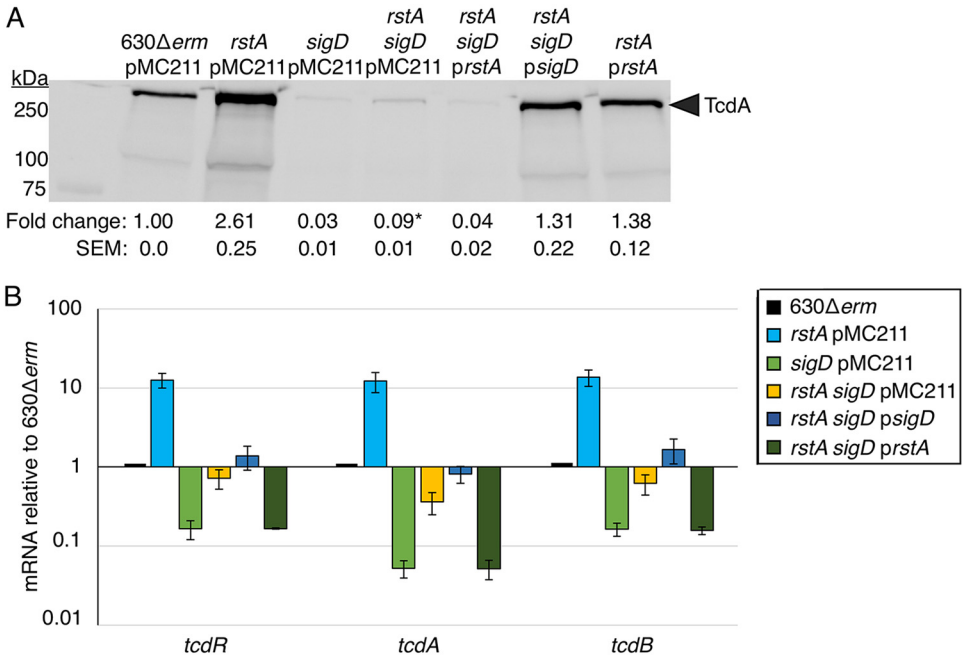

FIG 5 RstA represses toxin gene expression independently of SigD-mediated regulation. (A) Western blot analysis of TcdA in 630Δ*erm* pMC211 (MC282; vector control), *rstA* pMC211 (MC1224; vector control), *sigD*::*erm* pMC211 (MC506; vector control), *rstA sigD*::*erm* pMC211 (MC1281), *rstA sigD*::*erm* p*PcprA-rstA* (MC1282), *rstA sigD*::*erm* p*PcprA-sigD* (MC1283), and *rstA* p*PcprA-rstA* (MC1225) grown in TY medium (pH 7.4) supplemented with 2 μg/ml thiamphenicol and 1 μg/ml nisin, at 24 h. The corresponding image showing total protein is shown in Fig. S8A in the supplemental material. (B) qRT-PCR analysis of *tcdR*, *tcdA*, and *tcdB* transcript levels in 630Δ*erm* pMC211 (MC282; vector control), *rstA* pMC211 (MC1224; vector control), *sigD*::*erm* pMC211 (MC506; vector control), *rstA sigD*::*erm* pMC211 (MC1281), *rstA sigD*::*erm* p*PcprA-rstA* (MC1282), and *rstA sigD*::*erm* p*PcprA-sigD* (MC1283) grown in TY medium (pH 7.4) supplemented with 2 μg/ml thiamphenicol and 1 μg/ml nisin, at T_3 (three hours after the entry into stationary phase). The means and standard errors of the means for three biological replicates are shown. *, $P < 0.05$ by Student's *t* test between *sigD*::*erm* pMC211 and *rstA sigD*::*erm* pMC211.

CRISPR-Cas9 system modified for use in *C. difficile* to create an unmarked, nonpolar deletion of *rstA* in the 630Δ*erm* and *sigD*::*erm* backgrounds (Fig. S7) (40). TcdA protein levels were ~3-fold higher in the *rstA sigD* double mutant than in the *sigD* mutant (Fig. 5A; total protein loaded shown in Fig. S8A), indicating that RstA represses toxin production independently of SigD. Overexpression of *rstA* in the *rstA sigD* mutant returned TcdA protein to the levels found in the *sigD* mutant. Likewise, a previously characterized *sigD* overexpression construct (11, 41) restored TcdA to wild-type levels in the *rstA sigD* mutant, further supporting that SigD and RstA regulate toxin production independently (Fig. 5A). In addition, transcript levels of *tcdA*, *tcdB,* and *tcdR* were increased in the *rstA sigD* mutant compared to the levels in the *sigD* mutant (Fig. 5B), mirroring the TcdA protein results. Altogether, these data provide further evidence that RstA is major regulator of toxin production that directly and indirectly represses toxin gene expression independently of SigD.

RstA DNA-binding activity requires the species-specific C-terminal domains. The observation that RstA does not bind to target DNA in the tested *in vitro* conditions but does bind DNA in cell lysates suggests that a cofactor is required for RstA DNA-binding activity. We hypothesize that a small, quorum-sensing peptide serves as an activator for RstA DNA binding, as has been observed for other members of the RRNPP family (23–25, 42–44). To test this, we expressed RstA orthologs of other clostridial species (Fig. S9A) (45), including *Clostridium acetobutylicum*, *Clostridium perfringens*, and *Clostridium* (*Paeniclostridium*) *sordellii* in the *C. difficile rstA* mutant background. Only the *C. perfringens* RstA was stably produced in *C. difficile* (Fig. S9B). However, expression of the *C. perfringens rstA* ortholog failed to restore TcdA protein to wild-type levels (Fig. 6A; total protein loaded shown in Fig. S8B). *C. perfringens* RstA may be unable to repress *C.*

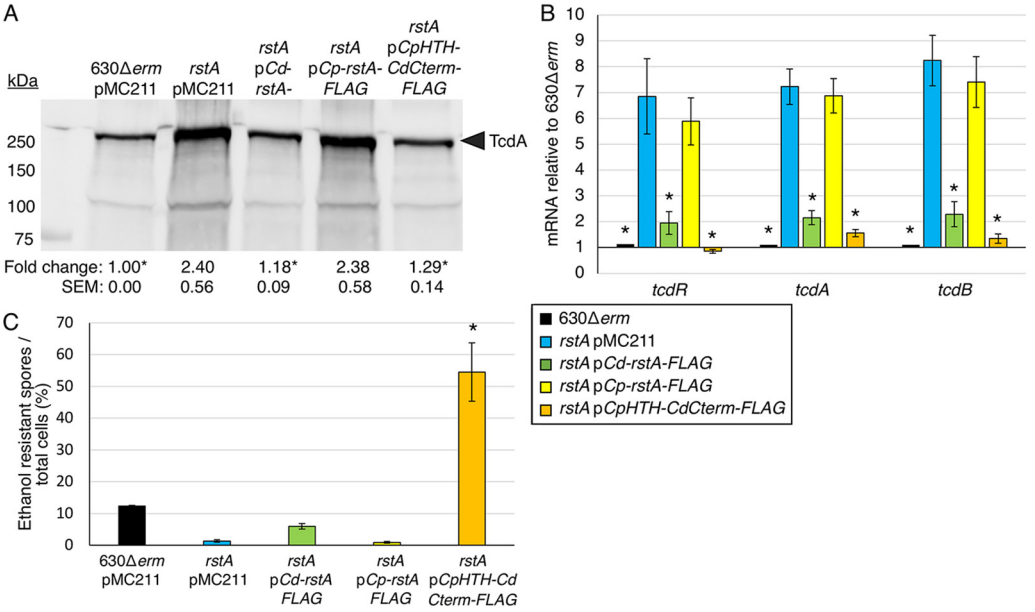

FIG 6 A hybrid *rstA* construct containing the *C. perfringens* DNA-binding domain with the *C. difficile* Spo0F-like and quorum-sensing-like domains complements *C. difficile rstA* toxin production and sporulation. (A) Western blot analysis of TcdA in 630Δ*erm* pMC211 (MC282; vector control), *rstA*::*erm* pMC211 (MC505; vector control), *rstA*::*erm* pP*cprA-rstA3XFLAG* (MC1004), *rstA*::*erm* pP*cprA-Cp-rstA3XFLAG* (MC1324), and *rstA*::*erm* pP*cprA-CpHTHCdCterminal3XFLAG* (MC1257) grown in TY medium, pH 7.4, supplemented with 2 μg/ml thiamphenicol and 1 μg/ml nisin, at H_{24}. The corresponding image showing total protein is shown in Fig. S8B. (B) qRT-PCR analysis of *tcdR*, *tcdA*, and *tcdB* transcript levels in 630Δ*erm* pMC211 (MC282; vector control), *rstA*::*erm* pMC211 (MC505; vector control), *rstA*::*erm* pP*cprA-rstA3XFLAG* (MC1004), *rstA*::*erm* pP*cprA-Cp-rstA3XFLAG* (MC1324), and *rstA*::*erm* pP*cprA-CpHTHCdCterminal3XFLAG* (MC1257) grown in TY medium, pH 7.4, supplemented with 2 μg/ml thiamphenicol and 1 μg/ml nisin, at T_3 (three hours after the entry into stationary phase). (C) Ethanol-resistant spore formation of 630Δ*erm* pMC211 (MC282; vector control), *rstA*::*erm* pMC211 (MC505; vector control), *rstA*::*erm* pP*cprA-rstA3XFLAG* (MC1004), *rstA*::*erm* pP*cprA-Cp-rstA3XFLAG* (MC1324), and *rstA*::*erm* pP*cprA-CpHTHCdCterminal3XFLAG* (MC1257) grown on 70:30 sporulation agar supplemented with 2 μg/ml thiamphenicol and 1 μg/ml nisin. Sporulation frequency is calculated as the number of ethanol-resistant spores divided by the total number of cells enumerated at H_{24} as detailed in Materials and Methods. The means and standard errors of the means for at least three independent biological replicates are shown; asterisks represent $P \leq 0.05$ by one-way ANOVA, followed by Dunnett's multiple-comparison test compared to *rstA* pMC211 (MC505).

difficile toxin production because the *C. perfringens* DNA-binding domain cannot recognize the *C. difficile* DNA target sequences and/or because the DNA-binding activity of *C. perfringens* RstA is not functional in *C. difficile*. To distinguish between these possibilities, we constructed a chimeric protein containing the *C. perfringens* DNA-binding domain (M1-Y51) fused to the C-terminal domains of the *C. difficile* RstA protein (herein known as *Cp*HTH-*Cd*CterminalFLAG) and examined the function of this chimeric RstA in the *C. difficile rstA* mutant. The RstA chimera restored *C. difficile* TcdA levels to those observed in the parent strain (Fig. 6A), indicating that the *C. perfringens* DNA-binding domain is functional in *C. difficile*. To confirm these results, we performed qRT-PCR analyses of *tcdR*, *tcdA*, and *tcdB* genes in these strains. The full-length *C. perfringens* RstA did not complement toxin gene expression in the *C. difficile rstA* mutant, while the *Cp*HTH-*Cd*Cterminal-FLAG chimeric RstA restored toxin gene transcript levels back to those observed in the parent strain (Fig. 6B), corroborating our previous results. These data strongly suggest that the C-terminal portion of RstA responds to species-specific signals to control the N-terminal DNA-binding activity.

Finally, we assessed the ability of a *C. perfringens* RstA to complement the low sporulation frequency of the *C. difficile rstA* mutant. Overexpressing the full-length *C. perfringens* RstA did not complement sporulation in the *C. difficile rstA* mutant (Fig. 6C). Unexpectedly, a hypersporulation phenotype was observed when the *Cp*HTH-*Cd*C-terminalFLAG RstA chimera was expressed in the *rstA* mutant (Fig. 6C), indicating that the chimeric *C. perfringens*-*C. difficile* RstA promotes *C. difficile* sporulation to even higher levels than the native *C. difficile* RstA does. This hypersporulation phenotype

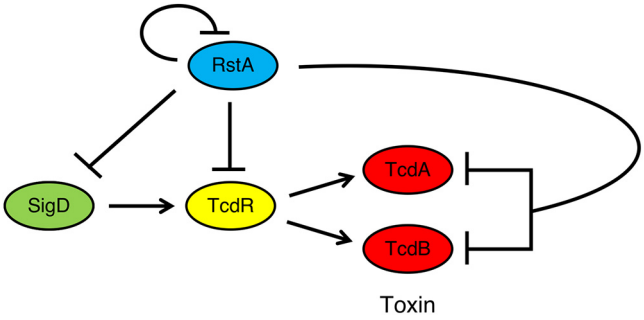

FIG 7 Model of RstA-mediated repression of *C. difficile* toxin production. SigD, the flagellum-specific sigma factor, directly induces gene transcription of *tcdR*, the toxin-specific sigma factor. Toxin gene expression is then directed by TcdR. RstA inhibits production of TcdA and TcdB and its own gene expression by directly binding to and repressing transcription of *sigD*, *tcdR*, *tcdA*, *tcdB*, and *rstA*, creating a complex, multitiered regulatory network to ensure that the toxin gene expression is appropriately timed in response to the signal(s) that activate RstA.

suggests that the *C. perfringens* HTH portion of the chimeric RstA protein alters the structure or activity of RstA to increase the positive effect on early sporulation events. These data warrant further investigation into the molecular mechanisms by which the C-terminal domains of RstA cooperate with the DNA-binding domain to promote sporulation.

DISCUSSION

The production of exotoxins and the ability to form quiescent endospores are two essential features of *C. difficile* pathogenesis. The regulatory links between toxin production and spore formation are complex and poorly understood. Some conserved sporulation regulatory factors, including Spo0A, CodY, and CcpA, strongly influence toxin production, yet some of these regulatory effects appear to be dependent on the strain or are indirect (8, 36, 46–48). Further, additional environmental conditions and metabolic signals, such as temperature and proline, glycine, and cysteine availability (5, 6, 10, 49), impact toxin production independently of these regulators, revealing the possibility that additional unknown factors are directly involved in toxin regulation (13). The recently discovered RRNPP regulator, RstA, represses toxin production and promotes spore formation, potentially providing a direct and inverse link between *C. difficile* spore formation and toxin biogenesis (14).

In this study, we show that RstA is a major, direct transcriptional regulator of *C. difficile* toxin gene expression. RstA inhibits toxin production by directly binding to the *tcdA* and *tcdB* promoters and repressing their transcription. RstA reinforces this repression by directly downregulating gene expression of *tcdR*, which encodes the sole sigma factor that drives *tcdA* and *tcdB* transcription. Finally, RstA directly represses the *flgB* promoter, inhibiting gene expression of the flagellum-specific sigma factor, SigD. SigD activates motility gene transcription but is also required for full expression of *tcdR* (11, 12). RstA repression of each major component in the toxin regulatory pathway creates a multitiered network in which RstA directly and indirectly controls *tcdA* and *tcdB* gene expression (Fig. 7).

RstA is the third characterized transcriptional repressor that directly binds to promoter regions for *tcdR*, *tcdA,* and *tcdB*, following two other transcriptional repressors, CodY and CcpA (8, 9, 36), The *in vivo* contribution of this reinforced repression of *tcdA* and *tcdB* transcription by CodY, CcpA, and RstA remains unknown. Interestingly, recent evidence has demonstrated that *tcdR* gene expression serves as a bistable switch that determines whether individual *C. difficile* cells within a population produce TcdA and TcdB, creating a divided population of toxin-OFF and toxin-ON cells (50). TcdR governs this bistability state by maintaining low basal expression levels, allowing for small changes to result in stochastic gene expression, and by positively regulating its own expression, establishing a positive-feedback loop that bolsters the toxin-ON state (50).

CodY was found to influence the population so that fewer cells produced toxin, but CcpA and RstA were not tested (50). We predict that both CcpA and RstA would bias the population of cells to a toxin-OFF state. Altogether, the tight control of *tcdR* transcription, reinforced by direct repression of *tcdA* and *tcdB* transcription by CcpA, CodY, and RstA, results in the convergence of multiple regulatory pathways at the bistable *tcdR* promoter to coordinate toxin production in response to nutritional and species-specific signals. This complex regulation ensures that the energy-intensive process of toxin production is initiated only to benefit the bacterium under the appropriate conditions.

Importantly, RstA is the first transcriptional regulator demonstrated to directly control *flgB* transcription initiation. To date, none of the previously identified regulators of *flgB* expression, including Spo0A, SigH, Agr, Hfq, SinR, and SinR′, have been shown to bind promoter DNA and regulate flagellar gene expression through transcription initiation (46, 51–54). *flgB* expression is further regulated posttranscriptionally via a c-di-GMP riboswitch and a flagellar switch, both of which are located within the large, 496-bp 5′ untranslated region (39, 55, 56); however, the impact of RstA-mediated repression of *flgB* gene expression through additional pathways has not yet been explored.

Although we have identified several direct RstA targets, the sequence required to recruit RstA to target promoters remains unclear. The *rstA* promoter contains a near-perfect inverted repeat; however, this sequence is AT rich, as is the case for many *C. difficile* promoters. Imperfect inverted repeats were also found overlapping the −35 consensus sequences of the *tcdA*, *tcdB*, *flgB*, and σ^A-dependent *tcdR* promoters, and immediately upstream of the σ^D-dependent *tcdR* promoter (Fig. S10) (57), suggesting that RstA inhibits transcription at these promoters by sterically obstructing RNA polymerase docking. No clear consensus sequence defining an RstA box is delineated from these sequences. Other RRNPP regulators have also been found to bind imperfect, palindromic repeats or specific, conserved sequences in target promoters, but to our knowledge, only PlcR has a defined binding motif (24, 58, 59). Exhaustive attempts at ChIP-seq analysis to identify the *C. difficile* RstA regulon proved unsuccessful; however, our data imply that RstA is a transcriptional repressor that directly controls multiple *C. difficile* phenotypes, and additional targets within the *C. difficile* genome seem likely.

The inability to recapitulate RstA-DNA binding with purified RstA *in vitro* together with the functional analysis of full-length and chimeric *C. difficile* and *C. perfringens* proteins suggest that (i) RstA DNA-binding activity requires a cofactor and (ii) this cofactor is species specific. Most RRNPP members are cotranscribed with their cognate quorum-sensing peptide precursor (19), but there are notable exceptions, including those encoded by unlinked genes (42, 60) and orphan receptors whose cognate ligands have not yet been discovered (61–63). RstA falls into this latter category, as there are no open reading frames adjacent to *rstA* that encode an apparent quorum-sensing peptide precursor. Importantly, no type of ligand other than small, quorum-sensing peptides has been identified for RRNPP proteins. In addition to RstA, other quorum-sensing factors have been implicated in *C. difficile* toxin production. The incomplete Agr1 and conserved Agr2 quorum-sensing systems induce toxin production through the production of a cyclic autoinducer peptide (AIP) that is sensed extracellularly (52, 64, 65); however, it is highly unlikely that the extracellular AIP molecule directly interacts with the cytosolic RstA protein. In addition, the interspecies LuxS-derived autoinducer-2 (AI-2) quorum-sensing molecule was found to increase *C. difficile tcdA* and *tcdB* gene expression, but not *tcdR* gene expression (66), indicating that AI-2 does not signal through RstA either. Identification of the cofactor that controls RstA activity is a high priority, as this will likely provide insight into the physiological conditions and/or metabolites that influence *C. difficile* TcdA and TcdB production.

Finally, as RstA is necessary for efficient *C. difficile* spore formation, the possibility remains that species-specific signaling is required for RstA-dependent control of early sporulation and that RstA coordinates *C. difficile* toxin production and spore formation in response to the same signal(s). Elucidating the molecular mechanisms that govern

TABLE 1 Bacterial strains and plasmids used in this study

Plasmid or strain	Relevant genotype or feature(s)	Source, construction, or reference
Plasmids		
pRK24	Tra$^+$ Mob$^+$ *bla, tet*	78
pJK02	*E. coli-C. difficile* shuttle vector; *catP*, *cas9*, *pyrE* sgRNA, *pyrE* homology region	40
pMC123	*E. coli-C. difficile* shuttle vector; *bla catP*	29
pMC211	pMC123 P*cprA*	77
pMC358	pMC123 ::*phoZ*	75
pMC367	pMC123 P*cprA-rstA* (*CD3668*)	14
pMC533	pMC123 P*cprA-rstA* (*C. sordellii* ATCC 9714)	This study
pMC543	pMC123 P*rstA*$_{489}$::*phoZ*	14
pMC559	pMC123 P*rstA*$_{A\text{-}27T}$::*phoZ*	This study
pMC560	pMC123 P*rstA*$_{T\text{-}23A}$::*phoZ*	This study
pMC561	pMC123 P*rstA*$_{T\text{-}19A}$::*phoZ*	This study
pMC562	pMC123 P*rstA*$_{A\text{-}18T}$::*phoZ*	This study
pMC563	pMC123 P*rstA*$_{T\text{-}17A}$::*phoZ*	This study
pMC573	pMC123 P*rstA*$_{A\text{-}27C}$::*phoZ*	This study
pMC574	pMC123 P*rstA*$_{A\text{-}24G}$::*phoZ*	This study
pMC575	pMC123 P*rstA*$_{A\text{-}21C}$::*phoZ*	This study
pMC576	pMC123 P*rstA*$_{T\text{-}19G}$::*phoZ*	This study
pMC660	pMC123 P*rstA*$_{115}$::*phoZ*	This study
pMC675	pMC123 P*cprA-rstA*-3XFLAG	This study
pMC676	pMC123 P*rstA*$_{IR}$(380 bp)::*phoZ*	This study
pMC677	pMC123 P*rstA*$_{231}$::*phoZ*	This study
pMC678	pMC123 P*rstA*$_{291}$::*phoZ*	This study
pMC682	pMC123 P*cprA-rstA*ΔHTH-3XFLAG	This study
pMC713	pMC123 P*tcdR*::*phoZ*	This study
pMC726	pJK02 with *rstA* homology region	This study
pMC729	pMC726 with *rstA* sgRNA (oMC1724)	This study
pMC752	pMC123 P*tcdR*(σ^A-92 bp)::*phoZ*	This study
pMC753	pMC123 P*tcdR*(σ^D)::*phoZ*	This study
pMC754	pMC123 P*tcdR*(P2 σ^{TcdR})::*phoZ*	This study
pMC755	pMC123 P*tcdR*(P1 σ^{TcdR})::*phoZ*	This study
pMC780	pMC123 P*cprA-rstA* (*C. perfringens* S13)	This study
pMC787	pMC123 P*cprA-rstA* (*C. acetobutylicum* ATCC 824)	This study
pMC795	pMC123 P*tcdA*::*phoZ*	This study
pMC796	pMC123 P*tcdB*::*phoZ*	This study
pMC798	pMC123 P*cprA-rstA*CpHTHCdCterminal-3XFLAG	This study
pMC812	pMC123 P*tcdR*(σ^A-76 bp)::*phoZ*	This study
pMC817	pRT1824 P*flgB* (630)::*phoZ*	This study
pMC818	pRT1824 P*flgB* (R20291)::*phoZ*	This study
pMC828	pMC123 P*cprA-rstA*-3XFLAG (*C. acetobutylicum* ATCC 824)	This study
pMC829	pMC123 P*cprA-rstA*-3XFLAG (*C. perfringens* S13)	This study
pMC830	pMC123 P*cprA-rstA*-3XFLAG (*C. sordellii* ATCC 9714)	This study
pMC888	pMC123 P*rstA*::*phoZ* P*cprA-rstA*-3XFLAG	This study
pMC889	pMC123 P*rstA*$_{T\text{-}19A/A\text{-}21C}$::*phoZ*	This study
pRPF144	pMLT960 P*cwp2-gusA*	79
pRT1824	pMLT960 ::*phoZ*	This study
pSigD	pMC123 P*cprA-sigD*	11
E. coli strains		
HB101 pRK24	F$^-$ *mcrB mrr hsdS20*(r_B^- m_B^-) *recA13 leuB6 ara-14 proA2 lacY1 galK2 xyl-5 mtl-1 rpsL20* pRK24	B. Dupuy
C. difficile strains		
630Δ*erm*	Erm^s derivative of strain 630	Nigel Minton; 80
MC282	630Δ*erm* pMC211	77
MC310	630Δ*erm spo0A*::*erm*	77
MC391	630Δ*erm rstA*::*erm*	14
MC448	630Δ*erm* pMC358	75
MC480	630Δ*erm rstA*::*erm* pMC367	14
MC505	630Δ*erm rstA*::*erm* pMC211	14
MC506	630Δ*erm sigD*::*erm* pMC211	This study
MC762	630Δ*erm rstA*::*erm* pMC533	This study
MC773	630Δ*erm* pMC543	14
MC774	630Δ*erm rstA*::*erm* pMC543	14

(Continued on next page)

TABLE 1 (Continued)

Plasmid or strain	Relevant genotype or feature(s)	Source, construction, or reference
MC830	630Δ*erm* pMC559	This study
MC831	630Δ*erm rstA*::*erm* pMC559	This study
MC832	630Δ*erm* pMC560	This study
MC833	630Δ*erm rstA*::*erm* pMC560	This study
MC834	630Δ*erm* pMC561	This study
MC835	630Δ*erm rstA*::*erm* pMC561	This study
MC836	630Δ*erm* pMC562	This study
MC837	630Δ*erm rstA*::*erm* pMC562	This study
MC838	630Δ*erm* pMC563	This study
MC839	630Δ*erm rstA*::*erm* pMC563	This study
MC856	630Δ*erm* pMC573	This study
MC857	630Δ*erm rstA*::*erm* pMC573	This study
MC858	630Δ*erm* pMC574	This study
MC859	630Δ*erm rstA*::*erm* pMC574	This study
MC860	630Δ*erm* pMC575	This study
MC861	630Δ*erm rstA*::*erm* pMC575	This study
MC862	630Δ*erm* pMC576	This study
MC863	630Δ*erm rstA*::*erm* pMC576	This study
MC979	630Δ*erm* pMC660	This study
MC980	630Δ*erm rstA*::*erm* pMC660	This study
MC1004	630Δ*erm rstA*::*erm* pMC675	This study
MC1008	630Δ*erm* pMC676	This study
MC1009	630Δ*erm rstA*::*erm* pMC676	This study
MC1010	630Δ*erm* pMC677	This study
MC1011	630Δ*erm rstA*::*erm* pMC677	This study
MC1012	630Δ*erm* pMC678	This study
MC1013	630Δ*erm rstA*::*erm* pMC678	This study
MC1028	630Δ*erm rstA*::*erm* pMC682	This study
MC1088	630Δ*erm* pMC713	This study
MC1089	630Δ*erm rstA*::*erm* pMC713	This study
MC1118	630Δ*erm* Δ*rstA*	This study
MC1133	630Δ*erm* pMC729	This study
MC1143	630Δ*erm* pMC752	This study
MC1144	630Δ*erm rstA*::*erm* pMC752	This study
MC1145	630Δ*erm* pMC753	This study
MC1146	630Δ*erm rstA*::*erm* pMC753	This study
MC1147	630Δ*erm* pMC754	This study
MC1148	630Δ*erm rstA*::*erm* pMC754	This study
MC1149	630Δ*erm* pMC755	This study
MC1150	630Δ*erm rstA*::*erm* pMC755	This study
MC1193	630Δ*erm sigD*::*erm* pMC729	This study
MC1224	630Δ*erm* Δ*rstA* pMC211	This study
MC1225	630Δ*erm* Δ*rstA* pMC367	This study
MC1249	630Δ*erm* pMC795	This study
MC1250	630Δ*erm rstA*::*erm* pMC795	This study
MC1251	630Δ*erm* pMC796	This study
MC1252	630Δ*erm rstA*::*erm* pMC796	This study
MC1257	630Δ*erm rstA*::*erm* pMC798	This study
MC1278	630Δ*erm* Δ*rstA sigD*::*erm*	This study
MC1281	630Δ*erm* Δ*rstA sigD*::*erm* pMC211	This study
MC1282	630Δ*erm* Δ*rstA sigD*::*erm* pMC367	This study
MC1283	630Δ*erm* Δ*rstA sigD*::*erm* pSigD	This study
MC1285	630Δ*erm* pMC812	This study
MC1286	630Δ*erm rstA*::*erm* pMC812	This study
MC1294	630Δ*erm* pMC817	This study
MC1295	630Δ*erm rstA*::*erm* pMC817	This study
MC1296	630Δ*erm* pMC818	This study
MC1297	630Δ*erm rstA*::*erm* pMC818	This study
MC1323	630Δ*erm rstA*::*erm* pMC828	This study
MC1324	630Δ*erm rstA*::*erm* pMC829	This study
MC1325	630Δ*erm rstA*::*erm* pMC830	This study
MC1433	630Δ*erm* pMC889	This study
MC1434	630Δ*erm rstA*::*erm* pMC889	This study

(Continued on next page)

TABLE 1 (Continued)

Plasmid or strain	Relevant genotype or feature(s)	Source, construction, or reference
MC1435	630Δ*erm rstA::erm* pMC888	This study
RT1075	630Δ*erm sigD::erm*	81
Other strains		
ATCC 824	*Clostridium acetobutylicum*	ATCC
ATCC 9714	*Clostridium sordellii*	ATCC

RstA activity will provide important insights into the regulatory control between sporulation and toxin production, reveal host cues and conditions that lead to increased toxin production, and help delineate the early sporulation events that control *C. difficile* Spo0A phosphorylation and activation.

MATERIALS AND METHODS

Bacterial strains and growth conditions. The bacterial strains and plasmids used in the study are listed in Table 1. *Clostridioides difficile* strains were routinely cultured in BHIS or TY medium (pH 7.4) supplemented with 2 to 5 μg/ml thiamphenicol and/or 1 μg/ml nisin throughout growth as needed (67). Overnight cultures of *C. difficile* were supplemented with 0.1% taurocholate and 0.2% fructose to promote spore germination and prevent sporulation, respectively, as indicated (67, 68). *C. difficile* strains were cultured in a 37°C anaerobic chamber with an atmosphere of 10% H_2, 5% CO_2, and 85% N_2, as previously described (69). *Escherichia coli* strains were grown at 37°C in LB (70) with 100 μg/ml ampicillin and/or 20 μg/ml chloramphenicol as needed. Kanamycin (50 μg/ml) was used for counterselection against *E. coli* HB101 pRK24 after conjugation with *C. difficile*, as previously described (71).

Strain and plasmid construction and accession numbers. Oligonucleotides used in this study are listed in Table 2. Details of vector construction are described in the supplemental material (see Fig. S1 in the supplemental material**)**. *C. difficile* strains 630 (GenBank accession no. NC_009089.1) and R20291 (GenBank accession no. FN545816.1), *Clostridium acetobutylicum* ATCC 824 (GenBank accession no. NC_003030.1), *Clostridium sordellii* ATCC 9714 (GenBank accession no. APWR00000000), and *Clostridium perfringens* S13 (GenBank accession no. BA000016.3) were used as the templates for primer design and PCR amplification. The *rstA* ortholog from *C. acetobutylicum* was synthesized by Genscript (Piscataway, NJ). The *Streptococcus pyogenes* CRISPR-Cas9 system, which has been modified for use in *C. difficile* (40), was used to create a nonpolar deletion of the *rstA* gene. The 630Δ*erm* and RT1075 (*sigD*::*erm*) strains containing the *rstA*-targeted CRISPR-Cas9 plasmid (MC1133 and MC1193, respectively) were grown overnight in TY medium with 5 μg/ml thiamphenicol. The next morning, the cultures were backdiluted into fresh TY medium supplemented with 5 μg/ml thiamphenicol and 100 ng/ml anhydrous tetracycline for 24 h to induce expression of the CRISPR-Cas9 system. A small aliquot of this culture was streaked onto BHIS plates, and colonies were screened by PCR for the presence or absence of the *rstA* allele.

Mapping the *rstA* transcriptional start with 5′ rapid amplification of cDNA ends (5′ RACE). DNase I-treated RNA from the *rstA*::*erm* mutant (MC391) was obtained as described above. 5′ RACE was performed using the 5′/3′ RACE kit, Second Generation (Roche), following the manufacturer's instructions as previously reported (72). Briefly, first strand cDNA synthesis was performed using the *rstA*-specific primer oMC982, followed by purification with the High Pure PCR Product purification kit (Roche). After subsequent poly(A) tailing of first strand cDNA, PCR amplification was performed using an oligo(T) primer and the *rstA*-specific primer oMC983 with Phusion DNA Polymerase (NEB). The resulting PCR products were purified from a 0.7% agarose gel (Qiagen) and TA cloned into pCR2.1 (Invitrogen) using the manufacturer's supplied protocols. Plasmids were isolated and sequenced (Eurofins MWG Operon) to determine the transcriptional start site (−32 bp from translational start site; $n = 7$).

Sporulation assays. *C. difficile* cultures were grown in BHIS medium supplemented with 0.1% taurocholate and 0.2% fructose until mid-exponential phase (i.e., an optical density at 600 nm [OD_{600}] of 0.5), and 0.25-ml portions were spotted onto 70:30 sporulation agar supplemented with 2 μg/ml thiamphenicol and 1 μg/ml nisin as a lawn (68). After 24 h growth, ethanol resistance assays were performed as previously described (73, 74). Briefly, the cells were scraped from plates after 24 h (H_{24}) and suspended in BHIS medium to an OD_{600} of 1.0. The total number of vegetative cells per milliliter was determined by immediately serially diluting and applying the resuspended cells to BHIS plates. Simultaneously, a 0.5-ml aliquot was mixed with 0.3 ml of 95% ethanol and 0.2 ml of dH_2O to achieve a final concentration of 28.5% ethanol, vortexed, and incubated for 15 min to eliminate all vegetative cells; ethanol-treated cells were subsequently serially diluted in 1× PBS plus 0.1% taurocholate and applied to BHIS plus 0.1% taurocholate plates to determine the total number of spores. After at least 36 h of growth, CFU were enumerated, and the sporulation frequency was calculated as the total number of spores divided by the total number of viable cells (spores plus vegetative cells). A *spo0A* mutant (MC310) was used as a negative sporulation control. Statistical significance was determined using a one-way ANOVA,

TABLE 2 Oligonucleotides used in this study[a]

Primer	Sequence (5'→3')	Use/locus tag/reference
oMC44	5' CTAGCTGCTCCTATGTCTCACATC	Forward primer for *rpoC* qPCR (29)
oMC45	5' CCAGTCTCTCCTGGATCAACTA	Reverse primer for *rpoC* qPCR (29)
oMC112	5' GGCAAATGTAAGATTTCGTACTCA	Forward primer for *tcdB* qPCR (77)
oMC113	5' TCGACTACAGTATTCTCTGAC	Forward primer for *tcdB* qPCR (77)
oMC352	5' GGAGTAGGTTTAGCTTTGTTATTAGGAACC	Forward primer for confirmation of *rstA* mutants
oMC547	5' TGGATAGGTGGAGAAGTCAGT	Forward primer for *tcdA* qPCR (77)
oMC548	5' GCTGTAATGCTTCAGTGGTAGA	Forward primer for *tcdA* qPCR (77)
oMC891	5' GCCATGGATCCAAAGGTGGGAATAGTATGGAAAT	Forward primer for *rstA*-3XFLAG constructs (14)
oMC982	5' TGGTCCTCAGCCTTGTTTAATTCAT	SP1 for *rstA* 5' RACE
oMC983	5' TGGCTTATTTGTGCTGCTGTTATCC	SP2 for *rstA* 5' RACE
oMC1006	5' GGAGCTTCCTCTTCTCTATCACTTA	Reverse primer for checking *sigD* mutation
oMC1136	5' GGCGAATTCGAGTAAATAGTAGCTGATTGAGC	Forward primer for P*rstA*(489 bp) reporter fusion (14)
oMC1137	5' GCCGGATCCACTATTCCCACCTTTTGAAGAC	Reverse primer for P*rstA* reporter fusions (14)
oMC1145	5' ATTCCAACAGTTCCTTTTCTCCTAAGCTCAAAATTTCC	Forward SOE primer for *rstA*-ΔHTH construct (14)
oMC1146	5' GCTTAGGAGAAAAGGAACTGTTGGAATATCTAGGCG	Reverse SOE primer for *rstA*-ΔHTH construct (14)
oMC1152	5' GCCATGGATCCTCTAGGGGGGCAGACATG	Forward primer for *C. sordellii* ATCC 9714 *rstA* (*ATCC9714_3891*)
oMC1153	5' GATGCCTGCAGCCCCCTAAAAACTTAATACTTATAA	Reverse primer for *C. sordellii* ATCC 9714 *rstA* (*ATCC9714_3891*)
oMC1204	5' TTCCACAACTTGCTGTTATTTCTC	Reverse primer for checking *rstA* mutants (14)
oMC1239	5' AAGTAGTGTTTTTTAAATAAATATAAGTTA	A-27T mutation in *rstA* promoter
oMC1240	5' TAACTTATATTTATTTAAAAAACACTACTT	A-27T mutation in *rstA* promoter
oMC1241	5' AAGTAGTGTTTTTAAAAAAAATATAAGTTA	T-23A mutation in *rstA* promoter
oMC1242	5' TAACTTATATTTTTTTTAAAAACACTACTT	T-23A mutation in *rstA* promoter
oMC1243	5' AAGTAGTGTTTTTAAAATAAAAATAAGTTA	T-19A mutation in *rstA* promoter
oMC1244	5' TAACTTATTTTTATTTTAAAAACACTACTT	T-19A mutation in *rstA* promoter
oMC1245	5' AAGTAGTGTTTTTAAAATAAATTTAAGTTA	A-18T mutation in *rstA* promoter
oMC1246	5' TAACTTAAATTTATTTTAAAAACACTACTT	A-18T mutation in *rstA* promoter
oMC1247	5' AAGTAGTGTTTTTAAAATAAATAAAAGTTA	T-17A mutation in *rstA* promoter
oMC1248	5' TAACTTTTATTTATTTTAAAAACACTACTT	T-17A mutation in *rstA* promoter
oMC1325	5' AAGTAGTGTTTTTCAAATAAATATAAGTTA	A-27C mutation in *rstA* promoter
oMC1326	5' TAACTTATATTTATTTGAAAAACACTACTT	A-27C mutation in *rstA* promoter
oMC1327	5' AAGTAGTGTTTTTAAAGTAAATATAAGTTA	A-24G mutation in *rstA* promoter
oMC1328	5' TAACTTATATTTACTTTAAAAACACTACTT	A-24G mutation in *rstA* promoter
oMC1329	5' AAGTAGTGTTTTTAAAATACATATAAGTTA	A-21C mutation in *rstA* promoter
oMC1330	5' TAACTTATATGTATTTTAAAAACACTACTT	A-21C mutation in *rstA* promoter
oMC1331	5' AAGTAGTGTTTTTAAAATAAAGATAAGTTA	T-19G mutation in *rstA* promoter
oMC1332	5' TAACTTATCTTTATTTTAAAAACACTACTT	T-19G mutation in *rstA* promoter
oMC1527	5' GGGAAATCATTTAATGTACAGTGAAAAT	Forward primer for P$rstA_{115}$; biotinylated
oMC1528	5' CATACTATTCCCACCTTTTGAAG	Reverse primer for P$rstA_{115}$
oMC1529	5' GTCAGAATTCGGGAAATCATTTAATGTACAGTGAAAAT	Forward primer for P$rstA_{115}$ reporter fusion

(Continued on next page)

TABLE 2 (Continued)

Primer	Sequence (5'→3')	Use/locus tag/reference
oMC1546	5' ATGCCTGCAGTCACTTGTCATCGTCATCCTTGTAATCT ATGTCATGATCTTTATAATCACCGTCATGGTCTTTGTAGT CGCTTCCCATTATTTCTAAGTTTTTGTACATAAATACACC	Reverse primer for RstA-3XFLAG
oMC1548	5' GACTCGGATCCCCCATAAAAATGACTAAAATTTAGTTT ATT	Reverse primer for P*rstA*$_{IR}$ (380 bp intergenic region) reporter fusion
oMC1549	5' GTCAGAATTCCTTATATATAATTATAGTCGTTATGAGCAA	Forward primer for P*rstA*$_{231}$ reporter fusion
oMC1550	5' GTCAGAATTCCTTAACACTAACATTATTTTCTTATTTTTC	Forward primer for P*rstA*$_{291}$ reporter fusion
oMC1611	5' CCCATAAAAATGACTAAAATTTAGTTTATT	Forward primer for P*rstA*$_{IR}$ (380 bp intergenic region); biotinylated
oMC1645	5' GGCGAATTCGGTTTCTAGATTTCATAAAAGATACTA	Forward primer for P*tcdR* reporter fusion
oMC1646	5' GCCGGATCCAAAATCATCCTCTCTTATATTTATAATG	Reverse primer for P*tcdR* reporter fusion
oMC1693	5' TGCTTTTAATGAAATTATTGTAAAAG	Forward primer for P*flgB*$_{630\Delta erm}$; biotinylated
oMC1694	5' GATATATTGTACAAATAAAATTGAAATATATGG	Forward primer for P*flgB*$_{R20291}$; biotinylated (RT1512)
oMC1695	5' AACTTAAGTATACAATAAATAACAAAT	Reverse primer for P*flgB*
oMC1724	5' CAATAAAGTGTGCTATAATTAAACTGTAAAGGTACCTGA AAGAATTAGCTGGAGATGTTTTAGAGCTAGAAATAGCAAGT TAAAATAAGGCTAGTCCGTTATCAACTTGAAAAAGTGGCAC CGAGTCGGTGCTTTTTTTCTATGGAGAAATCTAGATCAGCA TGATGTCTGACTAGACGCGTAAGCTCTGCAACTATTTTTAG ATGGTTGCA	*rstA* sgRNA sequence (underlined) within gBlock (IDT)
oMC1725	5' ATTGTTTCTATACCCTTATAGGTTTATTTACCACTATTCC CACCTTTTGAAGACATTT	Forward primer for *rstA* (5') homology region
oMC1726	5' ATTGTTTCTATACCCTTATAGGTTTATTTACCACTATTCC CACCTTTTGAAGACATTT	Reverse primer for *rstA* (5') homology region
oMC1727	5' AAATGTCTTCAAAAGGTGGGAATAGTGGTAAATAAACC TATAAGGGTATAGAAACAAT	Forward primer for *rstA* (3') homology region
oMC1728	5' GTGGGTCTGCGATCGCGCATGTCTGCAGGCCTCGAGT AAAAGTACATACTTAGGATAAGGTTTAGATTCTG	Reverse primer for *rstA* (3') homology region
oMC1733	5' GATTGATTAAGTTAAAAATGTGTATGTAA	Forward primer for P*tcdR*; biotinylated
oMC1734	5' AAAATCATCCTCTCTTATATTTATAATG	Reverse primer for P*tcdR*
oMC1753	5' CCTCCAATGTTAAAAAATAAACTGAG	Primer for sequencing gRNA in pMC729
oMC1762	5' TGACTGGGTTGAAGGCTCTCAAGGGCATCGGTCGACTGC TTTTAATGAAATTATTGTAAAAGAC	Forward primer for P*flgB* (630) reporter fusion
oMC1763	5' GCTCTTTTCTTCATTTCCTTGTTTCCTCCTGCATGCAACTT AAGTATACAATAAATAACAAATTTT	Reverse primer for P*flgB* (R20291) reporter fusion
oMC1766	5' TGACTGGGTTGAAGGCTCTCAAGGGCATCGGTCGACGAT ATATTGTACAAATAAAATTGAAATATATGG	Forward primer for P*flgB* (R20291) reporter fusion
oMC1768	5' CACGACGTTGTAAAACGACGGCCAGTATGAGAATTCGC CGATTATATAATTATAATGACTGA	Forward primer for P*tcdR*(σ^A) reporter fusion
oMC1769	5' TTCCTCCTTCATATCTACCCATACATTGACGGATCCAA AATCATCCTCTCTTATATTTATAATG	Reverse primer for P*tcdR*(σ^A) reporter fusion
oMC1770	5' CACGACGTTGTAAAACGACGGCCAGTATGAGAATTCGC TAAAATACTTTATTTATTAGAAAAAGATTA	Forward primer for P*tcdR*(σ^D) reporter fusion
oMC1771	5' TTCCTCCTTCATATCTACCCATACATTGACGGATCCCAT TATAATTATATAATCGGCAAATAAATT	Reverse primer for P*tcdR*(σ^D) reporter fusion
oMC1772	5' CACGACGTTGTAAAACGACGGCCAGTATGAGAATTCTG TTACTTGAAAATTGATCTATTTTAAA	Forward primer for P*tcdR*(P2σ^{TcdR}) reporter fusion
oMC1773	5' TTCCTCCTTCATATCTACCCATACATTGACGGATCCCTA ATAAATAAAGTATTTTAGCAATAAACT	Reverse primer for P*tcdR*(P2σ^{TcdR}) reporter fusion
oMC1774	5' CACGACGTTGTAAAACGACGGCCAGTATGAGAATTCGA TTGATTAAGTTAAAAATGTGTATGTAA	Forward primer for P*tcdR*(P1σ^{TcdR}) reporter fusion
oMC1804	5' TTCCTCCTTCATATCTACCCATACATTGACGGATCCAAT AGATCAATTTTCAAGTAACAATTA	Reverse primer for P*tcdR*(P1σ^{TcdR}) reporter fusion
oMC1841	5' ATAAGTTTGACAAAAGAAAGGATGAAAATTGGATCCGT AAGAGGATGATTTAAGCTATGG	Forward primer for *C. perfringens* S13 *rstA* (*CPE1448*)
oMC1842	5' TATGACCATGATTACGCCAAGCTTGCATGCCTGCAGGC TCTTTTTATTTTCTCCCCAG	Reverse primer for *C. perfringens* S13 *rstA* (*CPE1448*)
oMC1914	5' ATAAGTTTGACAAAAGAAAGGATGAAAATT	Forward primer for Gibson assembly into pMC211
oMC1915	5' TATGACCATGATTACGCCAAG	Reverse primer for Gibson assembly into pMC211
oMC1918	5' ATCCTTCAATGGATCTTTTAGAGTATCTAGGCGATAAGC TAGATGTAAGT	Forward primer for SOE PCR fusing the *rstA C. perfringens* DNA-binding domain with *C. difficile* C-terminal domains

(Continued on next page)

TABLE 2 (Continued)

Primer	Sequence (5'→3')	Use/locus tag/reference
oMC1919	5' ACTTACATCTAGCTTATCGCCTAGATACTCTAAAAGATC CATTGAAGGAT	Reverse primer for SOE PCR fusing the *rstA C. perfringens* DNA-binding domain with *C. difficile* C-terminal domains
oMC1929	5' CACGACGTTGTAAAACGACGGCCAGTATGAGAATTCTG GTCAGTTGGTAAAATCTATTAAG	Forward primer for P*tcdA* reporter fusion
oMC1930	5' TTCCTCCTTCATATCTACCCATACATTGACGGATCCAAA AACCTCCTAGTATTATTATTTTTGAT	Reverse primer for P*tcdA* reporter fusion
oMC1931	5' CACGACGTTGTAAAACGACGGCCAGTATGAGAATTCGT CTGTTTTTGAGGAAGATATTTG	Forward primer for P*tcdB* reporter fusion
oMC1932	5' TTCCTCCTTCATATCTACCCATACATTGACGGATCCCAT CTAAATGCTAAAACTCTTTTATATATC	Reverse primer for P*tcdB* reporter fusion
oMC1933	5' TATGACCATGATTACGCCAAGCTTGCATGCCTGCAGTC ACTTGTCATCGTCATCCTTGTAATCTATGTCATGATCTTTAT AATCACCGTCATGGTCTTTGTAGTCGCTTCCGATAATTTCTA AGTTTTGATATAAGCATAC	Reverse primer for *C. sordellii* ATCC 9714 *rstA* (*ATCC9714_3891*) with 3X-FLAG
oMC1934	5' TATGACCATGATTACGCCAAGCTTGCATGCCTGCAGTC ACTTGTCATCGTCATCCTTGTAATCTATGTCATGATCTTTAT AATCACCGTCATGGTCTTTGTAGTCGCTTCCACTTTTAATTA CACCTAAATTTTTCAG	Reverse primer for *C. perfringens* S13 *rstA* (*CPE1448*) with 3X-FLAG
oMC1935	5' TATGACCATGATTACGCCAAGCTTGCATGCCTGCAGTC ACTTGTCATCGTCATCCTTGTAATCTATGTCATGATCTTTAT AATCACCGTCATGGTCTTTGTAGTCGCTTCCCAAATCCTTCA ATACACCTATCTT	Reverse primer for *C. acetobutylicum* ATCC 824 *rstA* (*CA_C0957*) with 3X-FLAG
oMC1984	5' CACGACGTTGTAAAACGACGGCCAGTATGAGAATTCTAAT GACTGATTTAATTCCAATGTTG	Forward primer for P*tcdR*(P1σ^{TcdR}) 76 bp reporter fusion
oMC1977	5' CTCTTTTCTTCATTTCCTTGTTTCCTCCTGAATTCAACTTA AGTATACAATAAATAACAAATTT	Forward primer for site-directed mutagenesis of *Sph*I to *Eco*RI in pMC818
oMC1978	5' AAATTTGTTATTTATTGTATACTTAAGTTGAATTCAGGAGG AAACAAGGAAATGAAGAAAAGAG	Reverse primer for site-directed mutagenesis of *Sph*I to *Eco*RI in pMC818
oMC2193	5' AAGTAGTGTTTTTAAAATACAAATAAGTTA	T-19A/A-21C mutation in *rstA* promoter
oMC2194	5' TAACTTATTTGTATTTTAAAAACACTACTT	T-19A/A-21C mutation in *rstA* promoter
oMC2195	5' CACGACGTTGTAAAACGACGGCCAGTATGAGAATTCGAG TAAATAGTAGCTGATTGAGC	Forward primer for P*rstA*$_{T\text{-}19A/A\text{-}21C}$ mutation
oMC2196	5' TTCCTCCTTCATATCTACCCATACATTGACGGATCCACT ATTCCCACCTTTTGAAGAC	Reverse primer for P*rstA*$_{T\text{-}19A/A\text{-}21C}$ mutation
oMC2197	5' GTAAAACGACGGCCAGTATGAGAATTCTCACTTGTCATC GTCATCCTT	Forward primer for amplifying P*cprA-rstA-3XFLAG*
oMC2198	5' GCTCAATCAGCTACTATTTACTCGAATTCGACATGGAAGT AGAAGTTAAGG	Reverse primer for amplifying P*cprA-rstA-3XFLAG*
R1610	5' CAAGTTGGATCCCGTTCTGCTTTTTCTTCATTTTG	Reverse primer for amplifying *phoZ* (56)
R2282	5' GAATGCTAGCGAGCTGACTGGGTTGAAG	Forward primer for amplifying *phoZ*
sigDqF	5' GAATATGCCTCTTGTAAAGAGTATAGCA	Forward primer for checking *sigD* mutation (71)
tcdRqF	5' AGCAAGAAATAACTCAGTAGATGATT	Forward primer for *tcdR* qPCR (11)
tcdRqR	5' TTATTAAATCTGTTTCTCCCTCTTCA	Reverse primer for *tcdR* qPCR (11)

[a]Underlined nucleotides denote the restriction sites used for vector construction. Boldface red nucleotides indicate the bases mutated within the inverted repeat overlapping the *rstA* promoter.

followed by Dunnett's multiple-comparison test (GraphPad Prism v6.0), to compare sporulation efficiency to that of the *rstA* mutant.

Alkaline phosphatase activity assays. *C. difficile* strains containing the reporter fusions listed in Table 1 were grown and harvested on either 70:30 sporulation agar at H_8, defined as eight hours after the cultures are applied to the plates (early stationary phase), or from TY liquid medium in stationary phase (T_3, defined as three hours after the start of transition phase [approximately equivalent to H_8 on plates; early stationary phase], or H_{24}, defined as 24 h after the cultures are inoculated [late stationary phase]). Alkaline phosphatase assays were performed as described previously (75) with the exception that no chloroform was used for cell lysis. Technical duplicates were averaged, and the results are

presented as the means and standard errors of the means for three biological replicates. The two-tailed Student's *t* test was used to compare the activity in the *rstA* mutant to the activity in the parent strain.

Biotin pulldown assays. Biotin pulldown assays were performed as described by Jutras et al. (76). Briefly, a threefold excess of biotin-labeled DNA bait (30 μg) was coupled to streptavidin-coated magnetic beads (Invitrogen; binding capacity of 10 μg) in B/W buffer, and the bead-DNA complexes were washed with TE buffer to remove unbound DNA. In addition, an unbiotinylated P*rstA* (30 μg) negative control and a beads-only (dH_2O) negative control were treated alongside the test DNA fragments to ensure that RstA did not interact nonspecifically with the streptavidin-coated magnetic beads. To determine the total amount of biotinylated-DNA bound to each bead preparation, each incubation and subsequent washes were quantitated via a Nanodrop 1000 and subtracted from the initial amount of DNA. To prepare cell lysates, *C. difficile* expressing either RstA-FLAG (MC1004) or RstAΔHTH-FLAG (MC1028) in the *rstA* background were grown to mid-log phase (OD_{600} of 0.5 to 0.7) in 500 ml TY medium (pH 7.4) supplemented with 2 μg/ml thiamphenicol and 1 μg/ml nisin, pelleted, rinsed with sterile water, and stored at −80°C overnight. The pellets were suspended in 4.5 ml BS/THES buffer and lysed by cycling between a dry ice/ethanol bath and a 37°C water bath. The cell lysates were vortexed for 1 min to shear genomic DNA, and cell debris was pelleted at 15K rpm for 15 min at 4°C. The supernatant, along with 10 μg salmon sperm DNA as a nonspecific competitor, was then applied to the bead-DNA complexes and rotated for 30 min at room temperature. This incubation was repeated once with additional supernatant and 10 μg salmon sperm DNA for two total incubations. The bead-DNA-protein complexes were washed seven times with BS/THES buffer supplemented with 10 μg/ml salmon sperm DNA and then without salmon sperm DNA to remove nonspecific proteins. The beads were transferred to clean microcentrifuge tubes twice during the washes to eliminate carry-over contamination. The remaining bound protein was eluted with 250 mM NaCl in Tris-HCl, pH 7.4, and the eluates were immediately analyzed by SDS-PAGE and Western blotting using FLAG M2 antibody (Sigma; see below). Each DNA bait fragment was tested in at least three independent experiments. As a control following each experiment, bait DNA was recovered by incubating the labeled beads in dH_2O at 70°C for 10 min and analyzed on a 1.5% agarose gel to ensure that no cross-contamination occurred (data not shown). Densitometry was performed using Image Lab Software (Bio-Rad), and subsequent statistical analyses included a one-way ANOVA, followed by Dunnett's multiple-comparison test (GraphPad Prism v6.0).

Western blot analysis. The indicated *C. difficile* strains were grown in TY medium (pH 7.4) supplemented with 2 μg/ml thiamphenicol and 1 μg/ml nisin at 37°C and harvested at H_{24} (24 h) (74). Total protein was quantitated using the Pierce Micro BCA protein assay kit (Thermo Scientific), and 8 μg of total protein was separated by electrophoresis on a precast 4 to 15% TGX stain-free gradient gel (Bio-Rad), and total protein was imaged using a ChemiDoc (Bio-Rad). Corresponding gel images for each Western blot are included in the supplemental material as indicated in the text. Protein was then transferred to a 0.45-μm nitrocellulose membrane, and Western blot analysis was conducted with either mouse anti-TcdA (Novus Biologicals) or mouse anti-FLAG (Sigma) primary antibody, followed by goat anti-mouse Alexa Fluor 488 (Life Technologies) secondary antibody. Imaging and densitometry were performed with a ChemiDoc and Image Lab software (Bio-Rad), and a one-way ANOVA, followed by Dunnett's multiple-comparison test, was performed to assess statistical differences in TcdA protein levels between the *rstA* mutant and each *rstA* overexpression strain (GraphPad Prism v6.0). At least three biological replicates were analyzed for each strain, and a representative Western blot image is shown.

Quantitative reverse transcription-PCR analysis. *C. difficile* was cultivated in TY medium (pH 7.4) supplemented with 2 μg/ml thiamphenicol and 1 μg/ml nisin and harvested at T_3 (defined as three hours after the start of transition phase; OD_{600} of 1.0 [approximately equivalent to H_8 on plates]). Aliquots (3 ml) of culture were immediately mixed with 3 ml of ice-cold ethanol-acetone (1:1) and stored at −80°C. RNA was purified and DNase I treated (Ambion) as previously described (29, 35, 77), and cDNA was synthesized using random hexamers (77). Quantitative reverse transcription-PCR (qRT-PCR) analysis, using 50 ng cDNA per reaction and the SensiFAST SYBR & Fluorescein kit (Bioline), was performed in technical triplicates on a Roche Lightcycler 96. cDNA synthesis reaction mixtures containing no reverse transcriptase were included as a negative control to ensure that no genomic DNA contamination was present. Results are presented as the means and standard errors of the means for three biological replicates. Statistical significance was determined using a one-way ANOVA, followed by Dunnett's multiple-comparison test (GraphPad Prism v6.0), to compare transcript levels between the *rstA* mutant and each *rstA* overexpression strain.

SUPPLEMENTAL MATERIAL

Supplemental material for this article may be found at https://doi.org/10.1128/mBio.01991-18.

FIG S1, PDF file, 0.1 MB.
FIG S2, PDF file, 1.3 MB.
FIG S3, PDF file, 0.6 MB.
FIG S4, PDF file, 0.8 MB.
FIG S5, PDF file, 0.7 MB.
FIG S6, PDF file, 0.5 MB.
FIG S7, PDF file, 0.9 MB.
FIG S8, PDF file, 1.1 MB.

FIG S9, PDF file, 2.5 MB.
FIG S10, PDF file, 0.5 MB.

ACKNOWLEDGMENTS

We are grateful for the gift of *C. perfringens* S13 genomic DNA from Jorge Vidal. We give special thanks to Charles Moran and the members of McBride lab for helpful suggestions and discussions during the course of this work.

This research was supported by the U.S. National Institutes of Health through research grants AI116933 and AI121684 to S.M.M., AI107029 to R.T., and AI120613 to B.R.A.-F.

The contents of this article are solely the responsibility of the authors and do not necessarily reflect the official views of the National Institutes of Health.

REFERENCES

1. Rupnik M, Wilcox MH, Gerding DN. 2009. Clostridium difficile infection: new developments in epidemiology and pathogenesis. Nat Rev Microbiol 7:526–536. https://doi.org/10.1038/nrmicro2164.
2. Martin JS, Monaghan TM, Wilcox MH. 2016. Clostridium difficile infection: epidemiology, diagnosis and understanding transmission. Nat Rev Gastroenterol Hepatol 13:206–216. https://doi.org/10.1038/nrgastro.2016.25.
3. Kuehne SA, Cartman ST, Heap JT, Kelly ML, Cockayne A, Minton NP. 2010. The role of toxin A and toxin B in *Clostridium difficile* infection. Nature 467:711–713. https://doi.org/10.1038/nature09397.
4. Onderdonk AB, Lowe BR, Bartlett JG. 1979. Effect of environmental stress on Clostridium difficile toxin levels during continuous cultivation. Appl Environ Microbiol 38:637–641.
5. Karlsson S, Burman LG, Akerlund T. 1999. Suppression of toxin production in Clostridium difficile VPI 10463 by amino acids. Microbiology 145:1683–1693. https://doi.org/10.1099/13500872-145-7-1683.
6. Karlsson S, Lindberg A, Norin E, Burman LG, Akerlund T. 2000. Toxins, butyric acid, and other short-chain fatty acids are coordinately expressed and down-regulated by cysteine in Clostridium difficile. Infect Immun 68:5881–5888. https://doi.org/10.1128/IAI.68.10.5881-5888.2000.
7. Karlsson S, Burman LG, Akerlund T. 2008. Induction of toxins in Clostridium difficile is associated with dramatic changes of its metabolism. Microbiology 154:3430–3436. https://doi.org/10.1099/mic.0.2008/019778-0.
8. Dineen SS, Villapakkam AC, Nordman JT, Sonenshein AL. 2007. Repression of Clostridium difficile toxin gene expression by CodY. Mol Microbiol 66:206–219. https://doi.org/10.1111/j.1365-2958.2007.05906.x.
9. Antunes A, Martin-Verstraete I, Dupuy B. 2011. CcpA-mediated repression of Clostridium difficile toxin gene expression. Mol Microbiol 79:882–899. https://doi.org/10.1111/j.1365-2958.2010.07495.x.
10. Dubois T, Dancer-Thibonnier M, Monot M, Hamiot A, Bouillaut L, Soutourina O, Martin-Verstraete I, Dupuy B. 2016. Control of Clostridium difficile physiopathology in response to cysteine availability. Infect Immun 84:2389–2405. https://doi.org/10.1128/IAI.00121-16.
11. McKee RW, Mangalea MR, Purcell EB, Borchardt EK, Tamayo R. 2013. The second messenger cyclic di-GMP regulates Clostridium difficile toxin production by controlling expression of sigD. J Bacteriol 195:5174–5185. https://doi.org/10.1128/JB.00501-13.
12. El Meouche I, Peltier J, Monot M, Soutourina O, Pestel-Caron M, Dupuy B, Pons JL. 2013. Characterization of the SigD regulon of C. difficile and its positive control of toxin production through the regulation of tcdR. PLoS One 8:e83748. https://doi.org/10.1371/journal.pone.0083748.
13. Martin-Verstraete I, Peltier J, Dupuy B. 2016. The regulatory networks that control *Clostridium difficile* toxin synthesis. Toxins (Basel) 8:153. https://doi.org/10.3390/toxins8050153.
14. Edwards AN, Tamayo R, McBride SM. 2016. A novel regulator controls Clostridium difficile sporulation, motility and toxin production. Mol Microbiol 100:954–971. https://doi.org/10.1111/mmi.13361.
15. Mani N, Dupuy B. 2001. Regulation of toxin synthesis in Clostridium difficile by an alternative RNA polymerase sigma factor. Proc Natl Acad Sci U S A 98:5844–5849. https://doi.org/10.1073/pnas.101126598.
16. Aubry A, Hussack G, Chen W, KuoLee R, Twine SM, Fulton KM, Foote S, Carrillo CD, Tanha J, Logan SM. 2012. Modulation of toxin production by the flagellar regulon in Clostridium difficile. Infect Immun 80:3521–3532. https://doi.org/10.1128/IAI.00224-12.
17. Rocha-Estrada J, Aceves-Diez AE, Guarneros G, de la Torre M. 2010. The RNPP family of quorum-sensing proteins in Gram-positive bacteria. Appl Microbiol Biotechnol 87:913–923. https://doi.org/10.1007/s00253-010-2651-y.
18. Do H, Kumaraswami M. 2016. Structural mechanisms of peptide recognition and allosteric modulation of gene regulation by the RRNPP family of quorum-sensing regulators. J Mol Biol 428:2793–2804. https://doi.org/10.1016/j.jmb.2016.05.026.
19. Neiditch MB, Capodagli GC, Prehna G, Federle MJ. 2017. Genetic and structural analyses of RRNPP intercellular peptide signaling of Gram-positive bacteria. Annu Rev Genet 51:311–333. https://doi.org/10.1146/annurev-genet-120116-023507.
20. Perego M, Hoch JA. 1996. Cell-cell communication regulates the effects of protein aspartate phosphatases on the phosphorelay controlling development in Bacillus subtilis. Proc Natl Acad Sci U S A 93:1549–1553. https://doi.org/10.1073/pnas.93.4.1549.
21. Perego M. 1997. A peptide export-import control circuit modulating bacterial development regulates protein phosphatases of the phosphorelay. Proc Natl Acad Sci U S A 94:8612–8617. https://doi.org/10.1073/pnas.94.16.8612.
22. Jiang M, Grau R, Perego M. 2000. Differential processing of propeptide inhibitors of Rap phosphatases in Bacillus subtilis. J Bacteriol 182:303–310. https://doi.org/10.1128/JB.182.2.303-310.2000.
23. Slamti L, Lereclus D. 2002. A cell-cell signaling peptide activates the PlcR virulence regulon in bacteria of the Bacillus cereus group. EMBO J 21:4550–4559. https://doi.org/10.1093/emboj/cdf450.
24. Perchat S, Dubois T, Zouhir S, Gominet M, Poncet S, Lemy C, Aumont-Nicaise M, Deutscher J, Gohar M, Nessler S, Lereclus D. 2011. A cell-cell communication system regulates protease production during sporulation in bacteria of the Bacillus cereus group. Mol Microbiol 82:619–633. https://doi.org/10.1111/j.1365-2958.2011.07839.x.
25. Chang JC, LaSarre B, Jimenez JC, Aggarwal C, Federle MJ. 2011. Two group A streptococcal peptide pheromones act through opposing Rgg regulators to control biofilm development. PLoS Pathog 7:e1002190. https://doi.org/10.1371/journal.ppat.1002190.
26. Lereclus D, Agaisse H, Gominet M, Salamitou S, Sanchis V. 1996. Identification of a Bacillus thuringiensis gene that positively regulates transcription of the phosphatidylinositol-specific phospholipase C gene at the onset of the stationary phase. J Bacteriol 178:2749–2756. https://doi.org/10.1128/jb.178.10.2749-2756.1996.
27. Lazazzera BA, Kurtser IG, McQuade RS, Grossman AD. 1999. An autoregulatory circuit affecting peptide signaling in Bacillus subtilis. J Bacteriol 181:5193–5200.
28. Mashburn-Warren L, Morrison DA, Federle MJ. 2010. A novel double-tryptophan peptide pheromone controls competence in Streptococcus spp. via an Rgg regulator. Mol Microbiol 78:589–606. https://doi.org/10.1111/j.1365-2958.2010.07361.x.
29. McBride SM, Sonenshein AL. 2011. Identification of a genetic locus responsible for antimicrobial peptide resistance in Clostridium difficile. Infect Immun 79:167–176. https://doi.org/10.1128/IAI.00731-10.
30. Helmann JD. 1995. Compilation and analysis of Bacillus subtilis sigma A-dependent promoter sequences: evidence for extended contact between RNA polymerase and upstream promoter DNA. Nucleic Acids Res 23:2351–2360. https://doi.org/10.1093/nar/23.13.2351.

31. Moncrief JS, Barroso LA, Wilkins TD. 1997. Positive regulation of Clostridium difficile toxins. Infect Immun 65:1105–1108.
32. Mani N, Lyras D, Barroso L, Howarth P, Wilkins T, Rood JI, Sonenshein AL, Dupuy B. 2002. Environmental response and autoregulation of Clostridium difficile TxeR, a sigma factor for toxin gene expression. J Bacteriol 184:5971–5978. https://doi.org/10.1128/JB.184.21.5971-5978.2002.
33. Bouillaut L, Dubois T, Sonenshein AL, Dupuy B. 2015. Integration of metabolism and virulence in Clostridium difficile. Res Microbiol 166:375–383. https://doi.org/10.1016/j.resmic.2014.10.002.
34. Dupuy B, Sonenshein AL. 1998. Regulated transcription of Clostridium difficile toxin genes. Mol Microbiol 27:107–120. https://doi.org/10.1046/j.1365-2958.1998.00663.x.
35. Dineen SS, McBride SM, Sonenshein AL. 2010. Integration of metabolism and virulence by Clostridium difficile CodY. J Bacteriol 192:5350–5362. https://doi.org/10.1128/JB.00341-10.
36. Antunes A, Camiade E, Monot M, Courtois E, Barbut F, Sernova NV, Rodionov DA, Martin-Verstraete I, Dupuy B. 2012. Global transcriptional control by glucose and carbon regulator CcpA in Clostridium difficile. Nucleic Acids Res 40:10701–10718. https://doi.org/10.1093/nar/gks864.
37. Hammond GA, Lyerly DM, Johnson JL. 1997. Transcriptional analysis of the toxigenic element of Clostridium difficile. Microb Pathog 22:143–154. https://doi.org/10.1006/mpat.1996.0100.
38. Hundsberger T, Braun V, Weidmann M, Leukel P, Sauerborn M, von Eichel-Streiber C. 1997. Transcription analysis of the genes tcdA-E of the pathogenicity locus of Clostridium difficile. Eur J Biochem 244:735–742. https://doi.org/10.1111/j.1432-1033.1997.t01-1-00735.x.
39. Soutourina OA, Monot M, Boudry P, Saujet L, Pichon C, Sismeiro O, Semenova E, Severinov K, Le Bouguenec C, Coppee JY, Dupuy B, Martin-Verstraete I. 2013. Genome-wide identification of regulatory RNAs in the human pathogen Clostridium difficile. PLoS Genet 9:e1003493. https://doi.org/10.1371/journal.pgen.1003493.
40. McAllister KN, Bouillaut L, Kahn JN, Self WT, Sorg JA. 2017. Using CRISPR-Cas9-mediated genome editing to generate C. difficile mutants defective in selenoproteins synthesis. Sci Rep 7:14672. https://doi.org/10.1038/s41598-017-15236-5.
41. McKee RW, Aleksanyan N, Garrett EM, Tamayo R. 2018. Type IV pili promote Clostridium difficile adherence and persistence in a mouse model of infection. Infect Immun 86:e00943-17. https://doi.org/10.1128/IAI.00943-17.
42. Kozlowicz BK, Shi K, Gu ZY, Ohlendorf DH, Earhart CA, Dunny GM. 2006. Molecular basis for control of conjugation by bacterial pheromone and inhibitor peptides. Mol Microbiol 62:958–969. https://doi.org/10.1111/j.1365-2958.2006.05434.x.
43. Zouhir S, Perchat S, Nicaise M, Perez J, Guimaraes B, Lereclus D, Nessler S. 2013. Peptide-binding dependent conformational changes regulate the transcriptional activity of the quorum-sensor NprR. Nucleic Acids Res 41:7920–7933. https://doi.org/10.1093/nar/gkt546.
44. Cabrera R, Rodriguez-Romero A, Guarneros G, de la Torre M. 2016. New insights into the interaction between the quorum-sensing receptor NprR and its DNA target, or the response regulator Spo0F. FEBS Lett 590:3243–3253. https://doi.org/10.1002/1873-3468.12371.
45. Sievers F, Wilm A, Dineen D, Gibson TJ, Karplus K, Li W, Lopez R, McWilliam H, Remmert M, Soding J, Thompson JD, Higgins DG. 2011. Fast, scalable generation of high-quality protein multiple sequence alignments using Clustal Omega. Mol Syst Biol 7:539. https://doi.org/10.1038/msb.2011.75.
46. Deakin LJ, Clare S, Fagan RP, Dawson LF, Pickard DJ, West MR, Wren BW, Fairweather NF, Dougan G, Lawley TD. 2012. The *Clostridium difficile spo0A* gene is a persistence and transmission factor. Infect Immun 80:2704–2711. https://doi.org/10.1128/IAI.00147-12.
47. Nawrocki KL, Edwards AN, Daou N, Bouillaut L, McBride SM. 2016. CodY-dependent regulation of sporulation in Clostridium difficile. J Bacteriol 198:2113–2130. https://doi.org/10.1128/JB.00220-16.
48. Mackin KE, Carter GP, Howarth P, Rood JI, Lyras D. 2013. Spo0A differentially regulates toxin production in evolutionarily diverse strains of Clostridium difficile. PLoS One 8:e79666. https://doi.org/10.1371/journal.pone.0079666.
49. Karlsson S, Dupuy B, Mukherjee K, Norin E, Burman LG, Akerlund T. 2003. Expression of Clostridium difficile toxins A and B and their sigma factor TcdD is controlled by temperature. Infect Immun 71:1784–1793. https://doi.org/10.1128/IAI.71.4.1784-1793.2003.
50. Ransom EM, Kaus GM, Tran PM, Ellermeier CD, Weiss DS. 2018. Multiple factors contribute to bimodal toxin gene expression in Clostridioides (Clostridium) difficile. Mol Microbiol 110:533–549. https://doi.org/10.1111/mmi.14107.
51. Saujet L, Monot M, Dupuy B, Soutourina O, Martin-Verstraete I. 2011. The key sigma factor of transition phase, SigH, controls sporulation, metabolism, and virulence factor expression in Clostridium difficile. J Bacteriol 193:3186–3196. https://doi.org/10.1128/JB.00272-11.
52. Martin MJ, Clare S, Goulding D, Faulds-Pain A, Barquist L, Browne HP, Pettit L, Dougan G, Lawley TD, Wren BW. 2013. The agr locus regulates virulence and colonization genes in Clostridium difficile 027. J Bacteriol 195:3672–3681. https://doi.org/10.1128/JB.00473-13.
53. Boudry P, Gracia C, Monot M, Caillet J, Saujet L, Hajnsdorf E, Dupuy B, Martin-Verstraete I, Soutourina O. 2014. Pleiotropic role of the RNA chaperone protein Hfq in the human pathogen Clostridium difficile. J Bacteriol 196:3234–3248. https://doi.org/10.1128/JB.01923-14.
54. Girinathan BP, Ou J, Dupuy B, Govind R. 2018. Pleiotropic roles of Clostridium difficile sin locus. PLoS Pathog 14:e1006940. https://doi.org/10.1371/journal.ppat.1006940.
55. Sudarsan N, Lee ER, Weinberg Z, Moy RH, Kim JN, Link KH, Breaker RR. 2008. Riboswitches in eubacteria sense the second messenger cyclic di-GMP. Science 321:411–413. https://doi.org/10.1126/science.1159519.
56. Anjuwon-Foster BR, Tamayo R. 2017. A genetic switch controls the production of flagella and toxins in Clostridium difficile. PLoS Genet 13:e1006701. https://doi.org/10.1371/journal.pgen.1006701.
57. Rice P, Longden I, Bleasby A. 2000. EMBOSS: the European Molecular Biology Open Software Suite. Trends Genet 16:276–277. https://doi.org/10.1016/S0168-9525(00)02024-2.
58. Gohar M, Faegri K, Perchat S, Ravnum S, Okstad OA, Gominet M, Kolsto AB, Lereclus D. 2008. The PlcR virulence regulon of Bacillus cereus. PLoS One 3:e2793. https://doi.org/10.1371/journal.pone.0002793.
59. Lasarre B, Aggarwal C, Federle MJ. 2013. Antagonistic Rgg regulators mediate quorum sensing via competitive DNA binding in Streptococcus pyogenes. mBio 3:e00333-12. https://doi.org/10.1128/mBio.00333-12.
60. Folli C, Mangiarotti L, Folloni S, Alfieri B, Gobbo M, Berni R, Rivetti C. 2008. Specificity of the TraA-DNA interaction in the regulation of the pPD1-encoded sex pheromone response in Enterococcus faecalis. J Mol Biol 380:932–945. https://doi.org/10.1016/j.jmb.2008.05.058.
61. Even-Tov E, Omer Bendori S, Pollak S, Eldar A. 2016. Transient duplication-dependent divergence and horizontal transfer underlie the evolutionary dynamics of bacterial cell-cell signaling. PLoS Biol 14:e2000330. https://doi.org/10.1371/journal.pbio.2000330.
62. Makthal N, Gavagan M, Do H, Olsen RJ, Musser JM, Kumaraswami M. 2016. Structural and functional analysis of RopB: a major virulence regulator in Streptococcus pyogenes. Mol Microbiol 99:1119–1133. https://doi.org/10.1111/mmi.13294.
63. Parashar V, Konkol MA, Kearns DB, Neiditch MB. 2013. A plasmid-encoded phosphatase regulates Bacillus subtilis biofilm architecture, sporulation, and genetic competence. J Bacteriol 195:2437–2448. https://doi.org/10.1128/JB.02030-12.
64. Darkoh C, DuPont HL, Norris SJ, Kaplan HB. 2015. Toxin synthesis by Clostridium difficile is regulated through quorum signaling. mBio 6:e02569-14. https://doi.org/10.1128/mBio.02569-14.
65. Darkoh C, Odo C, DuPont HL. 2016. Accessory gene regulator-1 locus is essential for virulence and pathogenesis of Clostridium difficile. mBio 7:e01237-16. https://doi.org/10.1128/mBio.01237-16.
66. Lee AS, Song KP. 2005. LuxS/autoinducer-2 quorum sensing molecule regulates transcriptional virulence gene expression in Clostridium difficile. Biochem Biophys Res Commun 335:659–666. https://doi.org/10.1016/j.bbrc.2005.07.131.
67. Sorg JA, Dineen SS. 2009. Laboratory maintenance of Clostridium difficile. Curr Protoc Microbiol Chapter9:Unit9A.1. https://doi.org/10.1002/9780471729259.mc09a01s12.
68. Putnam EE, Nock AM, Lawley TD, Shen A. 2013. SpoIVA and SipL are Clostridium difficile spore morphogenetic proteins. J Bacteriol 195:1214–1225. https://doi.org/10.1128/JB.02181-12.
69. Edwards AN, Suarez JM, McBride SM. 2013. Culturing and maintaining *Clostridium difficile* in an anaerobic environment. J Vis Exp 2013(79):50787. https://doi.org/10.3791/50787.
70. Luria SE, Burrous JW. 1957. Hybridization between *Escherichia coli* and *Shigella*. J Bacteriol 74:461–476.
71. Purcell EB, McKee RW, McBride SM, Waters CM, Tamayo R. 2012. Cyclic diguanylate inversely regulates motility and aggregation in Clostridium difficile. J Bacteriol 194:3307–3316. https://doi.org/10.1128/JB.00100-12.
72. Woods EC, Nawrocki KL, Suarez JM, McBride SM. 2016. The Clostridium difficile Dlt pathway is controlled by the ECF sigma factor, sigmaV, in

response to lysozyme. Infect Immun 84:1902–1916. https://doi.org/10.1128/IAI.00207-16.
73. Edwards AN, McBride SM. 2017. Determination of the in vitro sporulation frequency of Clostridium difficile. Bio Protocol 7:e2125. https://doi.org/10.21769/BioProtoc.2125.
74. Childress KO, Edwards AN, Nawrocki KL, Woods EC, Anderson SE, McBride SM. 2016. The phosphotransfer protein CD1492 represses sporulation initiation in Clostridium difficile. Infect Immun 84:3434–3444. https://doi.org/10.1128/IAI.00735-16.
75. Edwards AN, Pascual RA, Childress KO, Nawrocki KL, Woods EC, McBride SM. 2015. An alkaline phosphatase reporter for use in *Clostridium difficile*. Anaerobe 32:98–104. https://doi.org/10.1016/j.anaerobe.2015.01.002.
76. Jutras BL, Verma A, Stevenson B. 2012. Identification of novel DNA-binding proteins using DNA-affinity chromatography/pull down. Curr Protoc Microbiol Chapter1:Unit1F.1. https://doi.org/10.1002/9780471729259.mc01f01s24.
77. Edwards AN, Nawrocki KL, McBride SM. 2014. Conserved oligopeptide permeases modulate sporulation initiation in *Clostridium difficile*. Infect Immun 82:4276–4291. https://doi.org/10.1128/IAI.02323-14.
78. Thomas CM, Smith CA. 1987. Incompatibility group P plasmids: genetics, evolution, and use in genetic manipulation. Annu Rev Microbiol 41:77–101. https://doi.org/10.1146/annurev.mi.41.100187.000453.
79. Fagan RP, Fairweather NF. 2011. Clostridium difficile has two parallel and essential Sec secretion systems. J Biol Chem 286:27483–27493. https://doi.org/10.1074/jbc.M111.263889.
80. Hussain HA, Roberts AP, Mullany P. 2005. Generation of an erythromycin-sensitive derivative of Clostridium difficile strain 630 (630Δerm) and demonstration that the conjugative transposon Tn916ΔE enters the genome of this strain at multiple sites. J Med Microbiol 54:137–141. https://doi.org/10.1099/jmm.0.45790-0.
81. Bordeleau E, Purcell EB, Lafontaine DA, Fortier LC, Tamayo R, Burrus V. 2015. Cyclic di-GMP riboswitch-regulated type IV pili contribute to aggregation of Clostridium difficile. J Bacteriol 197:819–832. https://doi.org/10.1128/JB.02340-14.